MATCH
Communications in Mathematical and in Computer Chemistry

MATCH Commun. Math. Comput. Chem. **90** (2023) 103–149
ISSN: 0340–6253
doi: 10.46793/match.90-1.103L

Exploration and Control of Bifurcation in a Fractional-Order Delayed Glycolytic Oscillator Model

Yizhong Liu

School of Mathematics and Statistics, Guizhou University of Finance and Economics, Guiyang 550025, PR China

liuyizhong151601@126.com

(Received November 19, 2022)

Abstract

Recently, establishing proper dynamical models to describe the relationship among different chemical substances has become a vital theme in chemistry. In this present article, we set up a new fractional-order delayed glycolytic oscillator model. Utilizing the contraction mapping theorem, we explore the existence and uniqueness of the solution to the involved fractional glycolytic oscillator model with delay. By virtue of some suitable analytical skills, we discuss the non-negativeness of the solution to the established fractional glycolytic oscillator system. Taking advantage of a suitable function, we investigate the boundedness of the fractional glycolytic oscillator system. Exploiting the stability and bifurcation theory of fractional dynamical system, we study the stability and the generation of Hopf bifurcation of the fractional glycolytic oscillator system with delay. Making use of delayed feedback controller and PD^{α} controller, we deal with the Hopf bifurcation control of the fractional glycolytic oscillator system owing delay. Computer simulation results are displayed to support the obtained assertions. The acquired results of this article own great theoretical value in dominating the concentrations of different chemical compositions.

1 Introduction

Applying mathematical tools to explore the dynamical behavior of chemical reaction models has become a vital topic in chemistry. In particular, in order to describe the changing relationship among different chemical compositions, differential dynamic system has become a common tool. How to set up a suitable dynamical model to describe the change law of different chemical compositions is a crucial aspect. In the past few decades, a great deal of chemical differential models have been established and fruitful results have been gained. For example, Khan [1] investigated the Neimark-Sacker bifurcation in a 2D discrete-time chemical dynamical model; Zafar et al. [2] dealt with the numerical modeling of a biochemical reaction model; Din and Haider [3] studied the Hopf bifurcation and chaos suppression in a Schnakenberg model; Kim et al. [4] discussed the positivity of a BGK model involving slow chemical reactions. Wang and Jia [5] explored the Hopf bifurcation and stability of a generalized Gray-Scott chemical reaction model; Wang et al. [6] dealt with the global dynamical trait of a stochastic chemostat model involving delays. For more related publications on this aspect, we refer the readers to [7–13].

In [14–16], the authors have investigated the following glycolytic oscillator model

$$\begin{cases} \dfrac{dv_1(t)}{dt} = a - bv_1(t) - v_1(t)v_2^2(t), \\ \dfrac{dv_2(t)}{dt} = bv_1(t) + v_1(t)v_2^2(t) - v_2(t), \end{cases} \tag{1}$$

where v_1 and v_1 stand for the concentration of fructose-6-phosphate and the concentration of adenosine diphosphate, respectively; $a > 0, b > 0$ are real numbers. For more concrete background of system (1), one can see [14–17].

Delay has a great influence on dynamics of differential dynamical systems. Usually, delay can make the dynamical system lose its stability, generate oscillation, emerge chaotic behavior and so on [18–20]. In system (1), the variation of the concentration of fructose-6-phosphate and the concentration of adenosine diphosphate depends upon the current time and the history time. That is to say, delay shall be appear in glycolytic oscillator

model. Based on this viewpoint, here we assume that the concentration of fructose-6-phosphate and the concentration of adenosine diphosphate owns the self-feedback delay, then we can amend system (1) as follows:

$$\begin{cases} \dfrac{dv_1(t)}{dt} = a - bv_1(t-\vartheta) - v_1(t)v_2^2(t), \\ \dfrac{dv_2(t)}{dt} = bv_1(t) + v_1(t)v_2^2(t) - v_2(t-\vartheta), \end{cases} \tag{2}$$

where $\vartheta > 0$ represents a delay.

During the recent decades, numerous researchers hold that fractional-order dynamical model can be considered a very valuable implement to depict the authentic natural law in object society than the integer-order ones because of the serious highlight of fractional-order dynamical model in the memory aspect and hereditary function of diverse substances and development process [21, 22]. Recently, fractional-order dynamical model has aroused great interest from lots of researchers due to its tremendous application aspect in complex networks, life sciences, neural networks, electronics, mechanics, secure cryptography, finance, artificial intelligence, chemistry and so on [23–28]. Currently, abundant results on fractional-order dynamical models have been acquired. For example, Yousef et al. [29] discussed the impact of fear in a fractional-order prey-predator model involving predator density-dependent prey mortality. Ghanbari and Djilali [30] carried out mathematical analysis on a fractional-order prey-predator model. Shafiya and Nagamani [31] set up a novel finite-time passivity criterion for a class of delayed fractional-order neural networks via Lyapunov function approach. Tan et al. [32] dealt with the event-triggered impulsive synchronization for a class of fractional-order coupled neural networks. Xu et al. [33] explored the Hopf bifurcation of fractional-order BAM neural networks with delays. In details, one can see [34–38]. Especially, delay-drived Hopf bifurcation of fractional-order dynamical systems is an important aspect in fractional-order dynamical systems. Exploring the impact of time delay on the stability and Hopf bifurcation behavior of fractional-order dynamical systems has aroused much interest form numerous researchers. Besides, dominating the stability region and the time of occurrence of Hopf bifurcation of fractional-order dynamical systems is

still a valuable work. Nowadays, some excellent works on Hopf bifurcation of fractional-order dynamical systems have been achieved (see [39–44]). However, there are merely very few publications dealing with the Hopf bifurcation of fractional-order chemical reaction models. What impact does the delay has on the dynamics of fractional-order chemical reaction models? How to build a proper controller to dominate the stability region and the time of the occurrence of Hopf bifurcation in such fractional-order chemical reaction models? We hope that these aspects can be effectively solved. Based on system (2) and the exploration above, we build the following fractional-order delayed glycolytic oscillator model and explore its Hopf bifurcation and Hopf bifurcation control aspect:

$$\begin{cases} \dfrac{d^{\alpha}v_1(t)}{dt^{\alpha}} = a - bv_1(t-\vartheta) - v_1(t)v_2^2(t), \\ \dfrac{d^{\alpha}v_2(t)}{dt^{\alpha}} = bv_1(t) + v_1(t)v_2^2(t) - v_2(t-\vartheta), \end{cases} \tag{3}$$

where $0 < \alpha \leq 1$.

The primary object of this article lie in the following aspects:

• Explore the stability and onset of Hopf bifurcation of the fractional-order delayed glycolytic oscillator model (3).

• Design two suitable controllers to control the stability region and the time of onset of Hopf bifurcation of the fractional-order delayed glycolytic oscillator model (3).

The key highlights of this work are presented as follows:

• Based on the earlier publications, a novel fractional-order delayed glycolytic oscillator model is set up.

• A new delay-dependent sufficient criterion guaranteeing the stability and occurrence of Hopf bifurcation of the fractional-order delayed glycolytic oscillator model (3) is derived. The influence of delay on the stability and bifurcation of the fractional-order delayed glycolytic oscillator model (3) is availably displayed.

• Proper delayed feedback controller and PD^{α} controller are designed to control the stability region and the time of occurrence of Hopf bifurcation of the fractional-order delayed glycolytic oscillator model (3).

• So far, the exploration on Hopf bifurcation and Hopf bifurcation control of the fractional-order delayed glycolytic oscillator model is very scarce.

The outline of this article is as follows. Section 2 lists the essential basic knowledge on fractional-order dynamical system. Section 3 explores the existence and uniqueness, non-negativeness and boundedness of the solution to system (3). Section 4 sets up a sufficient criterion about stability and Hopf bifurcation of system (3). Section 5 investigates the Hopf bifurcation control issue via delay feedback controller. Section 6 studies the Hopf bifurcation control issue via PD^{α} controller. Section 7 executes the computer simulations to validate the acquired chief conclusions. Section 8 draws a conclusion to complete this work.

2 Fundamental knowledge

In this passage, we are be about to provide some needful principles on fractional dynamical system.

Definition 2.1. **[45]** *Label the fractional integral of order α of the function $l(\nu)$ as follows*

$$\mathcal{I}^{\alpha} l(\nu) = \frac{1}{\Gamma(\alpha)} \int_{\nu_0}^{\nu} (\nu - s)^{\alpha - 1} l(s) ds,$$

where $\nu \geq \nu_0, \alpha > 0$, and $\Gamma(s) = \int_0^{\infty} \nu^{s-1} e^{-\nu} d\nu$ expresses the Gamma function.

Definition 2.2. **[45]** *Label $l(\nu) \in C([\nu_0, \infty), R)$. The Caputo-type fractional-order derivative of order α of $l(\nu)$ is given by:*

$$\mathcal{D}^{\alpha} l(\nu) = \frac{1}{\Gamma(l - \alpha)} \int_{\nu_0}^{\nu} \frac{l^{(m)}(s)}{(\alpha - s)^{\alpha - m + 1}} ds,$$

where $\nu \geq \nu_0$ and m is a positive integer obeying $m-1 \leq \alpha < m$. Especially, when $0 < \alpha < 1$, then

$$\mathcal{D}^{\alpha} l(\nu) = \frac{1}{\Gamma(1 - \alpha)} \int_{\nu_0}^{\nu} \frac{l^{'}(s)}{(\nu - s)^{\alpha}} ds.$$

Definition 2.3. **[46]** *Take into account the following fractional model:*

$$\mathcal{D}^{\alpha}v_i(t) = l_i(v_i(t)), i = 1, 2, \cdots, n, \tag{4}$$

where $\alpha \in (0, 1], v_i(t) = (v_1(t), v_2(t), \cdots, v_n(t)), l_i(t) = (l_1(t), l_2(t), \cdots, l_n(t))$. *Then we call* $(v_1^*, v_2^*, \cdots, v_n^*)$ *an equilibrium point of model (4) when* $l_i(v_i^*) = 0$.

Lemma 2.1. **[47]** *Label* $\alpha \in (0, 1]$ *and* $l(t) \in C[\epsilon_1, \epsilon_2]$ *and* $\mathcal{D}^{\alpha}l(t) \in C[\epsilon_1, \epsilon_2]$. *If* $\mathcal{D}^{\alpha}l(t) \geq 0, t \in (\epsilon_1, \epsilon_2)$, *then* $l(t)$ *is a non-decreasing function* $\forall \ \ t \in (\epsilon_1, \epsilon_2)$. *If* $\mathcal{D}^{\alpha}l(t) \leq 0, t \in (\epsilon_1, \epsilon_2)$, *then* $l(t)$ *is a non-increasing function* $\forall \ \ t \in (\epsilon_1, \epsilon_2)$.

Lemma 2.2. **[48]** *Take into account the fractional model* $\mathcal{D}^{\alpha}v = \mathcal{S}v$, $v(0) = v_0$ *where* $0 < \alpha < 1, v \in R^m, \mathcal{S} \in R^{m\times m}$. *Label* $\mu_l (l = 1, 2, \cdots, m)$ *the root of the characteristic equation of* $\mathcal{D}^{\alpha}v = \mathcal{S}v$. *Then the model* $\mathcal{D}^{\alpha}v = \mathcal{S}v$ *is asymptotically stable* $\Leftrightarrow |arg(\mu_l)| > \frac{\alpha\pi}{2} (l = 1, 2, \cdots, m)$. *Especially, this system is stable* $\Leftrightarrow |arg(\mu_l)| > \frac{\alpha\pi}{2} (l = 1, 2, \cdots, m)$ *and every critical eigenvalue satisfying* $|arg(\mu_l)| = \frac{\alpha\pi}{2} (l = 1, 2, \cdots, m)$ *owns geometric multiplicity one.*

Lemma 2.3. **[49]** *Take into account the fractional model* $\mathcal{D}^{\alpha}v(t) = \mathcal{S}_1v(t) + \mathcal{S}_2v(t - \tau)$, *where* $v(t) = \varpi(t), t \in [-\tau, 0], \alpha \in (0, 1], v \in R^m, \mathcal{S}_1, \mathcal{S}_2 \in R^{m\times m}$. *Then the characteristic equation of the model can be expressed as:* $\det|s^{\alpha}\mathcal{I} - \mathcal{S}_1 - \mathcal{S}_2e^{-s\tau}| = 0$. *Then the zero solution of the system is asymptotically stable provided that every root of the equation* $\det|s^{\alpha}\mathcal{I} - \mathcal{S}_1 - \mathcal{S}_2e^{-s\tau}| = 0$ *has negative real part.*

Lemma 2.4. **[50]** *Suppose that* $\phi(t) \in C[t_0, \infty)$ *and obeys*

$$\begin{cases} D^{\alpha}\varpi(t) \leq -r_1\varpi(t) + r_2, \\ \varpi(t_0) = \varpi_{t_0}, \end{cases}$$

where $\alpha \in (0, 1), r_1, r_2 \in R, r_1 \neq 0, t_0 \geq 0$, *then*

$$\varpi(t) \leq \left(\varpi(t_0) - \frac{r_2}{r_1}\right) E_{\alpha}[-r_1(t - t_0)^{\alpha}] + \frac{r_2}{r_1}.$$

3 Property of solution

In this section, we are going to explore the existence and uniqueness, non-negativeness of the solution to system (3).

Theorem 3.1. *Set* $\Delta = \{v_1, v_2) \in R^2 : \max\{|v_1|, |v_2|\} \leq \mathcal{V}\}$, *where* $\mathcal{V} > 0$ *implies a constant.* $\forall\ (v_{1\varsigma}, v_{2\varsigma}) \in \Delta$, *where* $\varsigma \in [\vartheta, t_0], t_0 > 0$ *is constant, the system (3) concerning the initial value* $(v_{1\varsigma}, v_{2\varsigma})$ *admits a unique solution* $V = (v_1, v_2) \in \Delta$.

Proof Label

$$\Pi(V) = (\Pi_1(V), \Pi_2(V)), \tag{5}$$

where

$$\begin{cases} \Pi_1(V) = a - bv_1(t-\vartheta) - v_1(t)v_2^2(t), \\ \Pi_2(V) = bv_1(t) + v_1(t)v_2^2(t) - v_2(t-\vartheta). \end{cases} \tag{6}$$

$\forall\ V, \tilde{V} \in \Delta$, one gains

$$\begin{aligned} &||\Pi(V) - \Pi(\tilde{V})|| = \big|a - bv_1(t-\vartheta) - v_1(t)v_2^2(t) \\ &-[a - b\tilde{v}_1(t-\vartheta) - \tilde{v}_1(t)\tilde{v}_2^2(t)]\big| \\ &+\big|bv_1(t) + v_1(t)v_2^2(t) - v_2(t-\vartheta) \\ &-[b\tilde{v}_1(t) + \tilde{v}_1(t)\tilde{v}_2^2(t) - \tilde{v}_2(t-\vartheta)]\big| \\ &\leq 2b\,|v_1(t-\vartheta) - \tilde{v}_1(t-\vartheta)| + |v_1(t)v_2^2(t) - \tilde{v}_1(t)\tilde{v}_2^2(t)| \\ &+|v_2(t-\vartheta) - \tilde{v}_2(t-\vartheta)| + |v_1(t)v_2^2(t) - \tilde{v}_1(t)\tilde{v}_2^2(t)| \\ &\leq 2b\,|v_1(t) - \tilde{v}_1(t)| + \mathcal{V}^2|v_1(t) - \tilde{v}_1(t)| + 2\mathcal{V}^2|v_2(t) - \tilde{v}_2(t)| \\ &+|v_2(t) - \tilde{v}_2(t)| + \mathcal{V}^2|v_1(t) - \tilde{v}_1(t)| + 2\mathcal{V}^2|v_2(t) - \tilde{v}_2(t)| \\ &= \left(2b + 2\mathcal{V}^2\right)|v_1(t) - \tilde{v}_1(t)| + (1 + 4\mathcal{V}^2)|v_2(t) - \tilde{v}_2(t)| \\ &\leq \kappa||V - \tilde{V}||, \end{aligned} \tag{7}$$

where

$$\kappa = \max\{2b + 2\mathcal{V}^2, 1 + 4\mathcal{V}^2\}. \tag{8}$$

Hence $\Pi(V)$ obeys Lipschitz condition regarding V (see [50]). Thus Theorem 3.1 holds. ■

Theorem 3.2. *Every solution to model (3) beginning from R_+^2 is nonnegative.*

Proof Label $V(t_0) = (V_1(t_0), V_2(t_0))$ the initial value of model (3). Suppose that $\exists$ a constant t_v satisfying $t_0 < t < t_v$ such that

$$\begin{cases} v_1(t) = 0, t_0 < t < t_v, \\ v_1(t_v) = 0, \\ v_1(t_v^+) < 0. \end{cases} \tag{9}$$

In the light of model (3), one gains

$$\mathcal{D}^\alpha v_1(t)|_{v_1(t_v)=0} = a > 0. \tag{10}$$

By Lemma 2.1, we can conclude that $v_a(t_v^+) > 0$, which contradicts model (3.5)(refer to [51]). Thus $v_a(t) \geq 0 \; \forall \;\; t \geq t_0$. In a same way, we can lightly verify that $v_2(t) \geq 0 \; \forall \;\; t \geq t_0$. ■

Theorem 3.3. *All solutions of model (3) beginning from R_+^2 are uniformly bounded.*

Label

$$W(t) = v_1(t) + v_2(t). \tag{11}$$

Then

$$\begin{aligned} \mathcal{D}^\alpha W(t) &= \mathcal{D}^\alpha v_1(t) + \mathcal{D}^\alpha v_2(t) \\ &= a - bv_1(t-\vartheta) - v_1(t)v_2^2(t) \\ &+ bv_1(t) + v_1(t)v_2^2(t) - v_2(t-\vartheta) \\ &= -bv_1(t-\vartheta) - v_2(t-\vartheta) + a + b\mathcal{V} \\ &\leq -\min\{b, 1\}W(t) + a + b\mathcal{V}, \end{aligned} \tag{12}$$

which results in

$$\mathcal{D}^\alpha W(t) + \min\{b, 1\}W(t) \leq a + b\mathcal{V}. \tag{13}$$

In view of Lemma 2.4, one gains

$$W(t) \leq \left(W(t_0) - \frac{a + b\mathcal{V}}{\min\{b, 1\}} \right) E_\alpha[-\min\{b, 1\}(t - t_0)^\alpha] + \frac{a + b\mathcal{V}}{\min\{b, 1\}}, \quad (14)$$

then

$$W(t) \to \frac{a + b\mathcal{V}}{\min\{b, 1\}}, \text{ as } t \to \infty. \quad (15)$$

The proof of Theorem 3.3 comes to an end. ■

4 Bifurcation discussion of model (3)

In this part, we are about to deal with the stability trait and bifurcation phenomenon of model (3). Obviously, model (3) admits one positive equilibrium point $E(v_{1*}, v_{2*})$. where

$$\begin{cases} v_{1*} = \dfrac{a}{b + a^2}, \\ v_{2*} = a. \end{cases} \quad (16)$$

Label

$$\begin{cases} \bar{v}_1(t) = v_1(t) - v_{1*}, \\ \bar{v}_2(t) = v_2(t) - v_{2*}, \end{cases} \quad (17)$$

then

$$\begin{cases} v_1(t) = \bar{v}_1(t) + v_{1*}, \\ v_2(t) = \bar{v}_2(t) + v_{2*}. \end{cases} \quad (18)$$

Applying (18) and (3) brings about

$$\begin{cases} \dfrac{d^\alpha \bar{v}_1(t)}{dt^\alpha} = a - b[\bar{v}_1(t - \vartheta) + v_{1*}] - (\bar{v}_1(t) + v_{1*})(\bar{v}_2(t) + v_{2*})^2 \\ \dfrac{d^\alpha \bar{v}_2(t)}{dt^\alpha} = b(\bar{v}_1(t) + v_{1*}) + (\bar{v}_1(t) + v_{1*})(\bar{v}_2(t) + v_{2*})^2 \\ \qquad\qquad - [\bar{v}_2(t - \vartheta) + v_{2*}]. \end{cases} \quad (19)$$

Linearizing system (19) at $(0,0)$ leads to

$$\begin{cases} \dfrac{d^{\alpha}\bar{v}_1(t)}{dt^{\alpha}} = -v_{2*}^2\bar{v}_1(t) - 2v_{1*}v_{2*}\bar{v}_2(t) - b\bar{v}_1(t-\vartheta), \\ \dfrac{d^{\alpha}\bar{v}_2(t)}{dt^{\alpha}} = (b+v_{2*}^2)\bar{v}_1(t) + 2v_{1*}v_{2*}\bar{v}_2(t) - \bar{v}_2(t-\vartheta). \end{cases} \tag{20}$$

The characteristic equation of Eq. (20) is given by

$$\det\begin{bmatrix} s^{\alpha} + v_{2*}^2 - be^{-s\vartheta} & 2v_{1*}v_{2*} \\ -(b+v_{2*}^2) & s^{\alpha} - 2v_{1*}v_{2*} + e^{-s\vartheta} \end{bmatrix} = 0, \tag{21}$$

which brings about

$$s^{2\alpha} + \alpha_1 s^{\alpha} + \alpha_2 + (\alpha_3 s^{\alpha} + \alpha_4)e^{-s\vartheta} + \alpha_5 e^{-2s\vartheta} = 0, \tag{22}$$

where

$$\begin{cases} \alpha_1 = v_{2*}^2 - 2v_{1*}v_{2*}, \\ \alpha_2 = 2bv_{1*}v_{2*}, \\ \alpha_3 = -b, \\ \alpha_4 = 2bv_{1*}v_{2*} + v_{2*}^2, \\ \alpha_5 = -b. \end{cases} \tag{23}$$

The following essential hypothesis is provided:

$$(Q_1)\quad \alpha_1 + \alpha_3 > 0, \alpha_2 + \alpha_4 + \alpha_5 > 0.$$

Lemma 4.1. *Provided that* (Q_1) *holds, then the positive equilibrium point* $E(v_{1*}, v_{2*})$ *of model (3) is locally asymptotically stable.*

Proof If $\vartheta = 0$, then Eq.(22) turns into:

$$\lambda^2 + (\alpha_1 + \alpha_3)\lambda + \alpha_2 + \alpha_4 + \alpha_5 = 0. \tag{24}$$

In the light of (Q_1), the double roots λ_1 and λ_1 of (24) satify $|\arg(\lambda_1)| > \frac{\alpha\pi}{2}, |\arg(\lambda_2)| > \frac{\alpha\pi}{2}$. Exploiting Lemma 2.2, one can understand that the positive equilibrium point $E(v_{1*}, v_{2*})$ of model (3) is locally asymptotically stable. The proof comes to an end. ■

Now we rewrite Eq.(22) as

$$(s^{2\alpha}+\alpha_1 s^{\alpha}+\alpha_2)e^{s\alpha}+\alpha_3 s^{\alpha}+\alpha_4+\alpha_5 e^{-s\alpha}=0. \tag{25}$$

Label $s=i\varrho=\varrho\left(\cos\frac{\pi}{2}+i\sin\frac{\pi}{2}\right)$ the root of Eq.(25). Then

$$\left[\varrho^{2\alpha}(\cos\alpha\pi+i\sin\alpha\pi)+\alpha_1\varrho^{\alpha}\left(\cos\frac{\alpha\pi}{2}+i\sin\frac{\alpha\pi}{2}\right)+\alpha_2\right]$$

$$\times(\cos\varrho\vartheta+i\sin\varrho\vartheta)+\alpha_3\varrho^{\alpha}\left(\cos\frac{\alpha\pi}{2}+i\sin\frac{\alpha\pi}{2}\right)$$

$$+\alpha_4+\alpha_5(\cos\varrho\vartheta-i\sin\varrho\vartheta)=0, \tag{26}$$

which brings about

$$\begin{cases} b_1\cos\varrho\vartheta-b_2\sin\varrho\vartheta=b_3,\\ b_2\cos\varrho\vartheta+b_4\sin\varrho\vartheta=b_5, \end{cases} \tag{27}$$

where

$$\begin{cases} b_1=c_1\varrho^{2\alpha}+c_2\varrho^{\alpha}+c_3,\\ b_2=c_4\varrho^{2\alpha}+c_5\varrho^{\alpha},\\ b_3=c_6\varrho^{\alpha}+c_7,\\ b_4=c_1\varrho^{2\alpha}+c_2\varrho^{\alpha}+c_8,\\ b_5=c_9\varrho^{\alpha}, \end{cases} \tag{28}$$

where

$$\begin{cases} c_1=\cos\alpha\pi,\\ c_2=\alpha_1\cos\frac{\alpha\pi}{2},\\ c_3=\alpha_2+\alpha_5,\\ c_4=\sin\alpha\pi,\\ c_5=\alpha_1\sin\frac{\alpha\pi}{2},\\ c_6=-\alpha_3\cos\frac{\alpha\pi}{2},\\ c_7=-\alpha_4,\\ c_8=\alpha_2-\alpha_5,\\ c_9=-\alpha_3\sin\frac{\alpha\pi}{2}. \end{cases} \tag{29}$$

In view of (27), one gains

$$\begin{cases} \cos \varrho\vartheta = \dfrac{b_3b_4 + b_2b_5}{b_1b_4 + b_2^2}, \\ \sin \varrho\vartheta = \dfrac{b_1b_5 - b_2b_3}{b_1b_4 + b_2^2} \end{cases} \tag{30}$$

and

$$(b_3b_4 + b_2b_5)^2 + (b_1b_5 - b_2b_3)^2 = (b_1b_4 + b_2^2)^2. \tag{31}$$

Using (31), one gains

$$\eta_1\varrho^{8\alpha} + \eta_2\varrho^{7\alpha} + \eta_3\varrho^{6\alpha} + \eta_4\varrho^{5\alpha} + \eta_5\varrho^{4\alpha} + \eta_6\varrho^{3\alpha} + \eta_7\varrho^{2\alpha} + \eta_8\varrho^{\alpha} + \eta_9 = 0, \tag{32}$$

where

$$\begin{cases} \eta_1 = (c_1^2 + c_4^2)^2, \\ \eta_2 = 4(c_1^2 + c_4^2)^2(c_1c_2 + c_4c_5), \\ \eta_3 = 4(c_1c_2 + c_4c_5)^2 + 2(c_1^2 + c_4^2)(c_1c_8 + c_1c_3 + c_2^2 + c_5^2) \\ \qquad - (c_1c_6 + c_4c_6)^2 - (c_1c_9 - c_4c_6)^2, \\ \eta_4 = 2(c_1^2 + c_4^2)(c_2c_8 + c_2c_3) \\ \qquad - 2(c_1c_6 + c_4c_6)(c_2c_6 + c_5c_6 + c_1c_7) \\ \qquad - 2(c_1c_9 - c_4c_6)(c_2c_9 - c_4c_7 - c_5c_6), \\ \eta_5 = (c_1c_8 + c_1c_3 + c_2^2 + c_5^2)^2 + 4(c_1c_2 + c_4c_5)(c_2c_8 + c_2c_3), \\ \qquad - (c_2c_6 + c_5c_6 + c_1c_7)^2 - 2(c_1c_6 + c_4c_6)(c_6c_8 + c_2c_7) \\ \qquad - (c_2c_9 - c_4c_7 - c_5c_6)^2 - 2(c_1c_9 - c_4c_6)(c_3c_9 - c_5c_7), \\ \eta_6 = 4c_3c_8(c_1c_2 + c_4c_5) + 2(c_1c_8 + c_1c_3 + c_2^2 + c_5^2)(c_2c_8 + c_2c_3) \\ \qquad - 2c_7c_8(c_1c_6 + c_4c_6) - 2(c_2c_6 + c_5c_6 + c_1c_7)(c_6c_8 + c_2c_7) \\ \qquad - 2(c_2c_9 - c_4c_7 - c_5c_6)(c_3c_9 - c_5c_7), \\ \eta_7 = 2c_3c_8(c_1c_8 + c_1c_3 + c_2^2 + c_5^2) + (c_2c_8 + c_2c_3)^2 \\ \qquad - (c_6c_8 + c_2c_7)^2 - 2c_7c_8(c_2c_6 + c_5c_6 + c_1c_7) \\ \qquad - (c_3c_9 - c_5c_7)^2, \\ \eta_8 = 2c_3c_8(c_2c_8 + c_2c_3) - 2c_7c_8(c_6c_8 + c_2c_7), \\ \eta_9 = (c_3c_8)^2 - (c_7c_8)^2. \end{cases} \tag{33}$$

Label

$$\Theta_1(\varrho) = \eta_1\varrho^{8\alpha} + \eta_2\varrho^{7\alpha} + \eta_3\varrho^{6\alpha} + \eta_4\varrho^{5\alpha}$$

$$+\eta_5\varrho^{4\alpha}+\eta_6\varrho^{3\alpha}+\eta_7\varrho^{2\alpha}+\eta_8\varrho^{\alpha}+\eta_9. \tag{34}$$

Suppose that

$$(Q_2)\ |c_3|<|c_7|$$

is fulfilled, consider that $\frac{d\Theta_1(\varrho)}{d\varrho}>0,\ \forall\ \ \varrho>0$, then one easily know that Eq.(32) admits at the very least one positive real root. Hence Eq.(25) admits at the very least one couple of purely roots.

Suppose that Eq.(32) admits eight real roots (say $\varrho_j>0(j=1,2,\cdots,8)$. In conformity with (30), one gains

$$\vartheta_j^h=\frac{1}{\varrho_i}\left[\arccos\left(\frac{b_3b_4+b_2b_5}{b_1b_4+b_2^2}\right)+2h\pi\right], \tag{35}$$

where $h=0,1,2,\cdots,j=1,2,\cdots,8$. Label

$$\vartheta_0=\min_{j=1,2,\cdots,8}\{\vartheta_j^0\},\varrho_0=\varrho|_{\vartheta=\vartheta_0}. \tag{36}$$

Now we list the following indispensable hypothesis:

$(Q_3)\ \ U_1M_1+U_2M_2>0$, where

$$\begin{cases}
U_1=2\alpha\varrho_0^{2\alpha-1}\cos\dfrac{(2\alpha-1)\pi}{2}+\alpha_1\alpha\varrho_0^{\alpha-1}\cos\dfrac{(\alpha-1)\pi}{2}\\
\qquad+\alpha_3\alpha\varrho_0^{\alpha-1}\cos\dfrac{(\alpha-1)\pi}{2}\cos\varrho_0\vartheta_0\\
\qquad+\alpha_3\alpha\varrho_0^{\alpha-1}\sin\dfrac{(\alpha-1)\pi}{2}\sin\varrho_0\vartheta_0,\\
U_2=2\alpha\varrho_0^{2\alpha-1}\sin\dfrac{(2\alpha-1)\pi}{2}+\alpha_1\alpha\varrho_0^{\alpha-1}\sin\dfrac{(\alpha-1)\pi}{2}\\
\qquad-\alpha_3\alpha\varrho_0^{\alpha-1}\cos\dfrac{(\alpha-1)\pi}{2}\sin\varrho_0\vartheta_0\\
\qquad+\alpha_3\alpha\varrho_0^{\alpha-1}\sin\dfrac{(\alpha-1)\pi}{2}\cos\varrho_0\vartheta_0,\\
M_1=\left(\alpha_3\varrho_0^{\alpha}\cos\dfrac{\alpha\pi}{2}+\alpha_4\right)\varrho_0\sin\varrho_0\vartheta_0\\
\qquad-\left(\alpha_3\varrho_0^{\alpha}\sin\dfrac{\alpha\pi}{2}\right)\varrho_0\cos\varrho_0\vartheta_0,\\
M_2=\left(\alpha_3\varrho_0^{\alpha}\cos\dfrac{\alpha\pi}{2}+\alpha_4\right)\varrho_0\cos\varrho_0\vartheta_0\\
\qquad+\left(\alpha_3\varrho_0^{\alpha}\sin\dfrac{\alpha\pi}{2}\right)\varrho_0\sin\varrho_0\vartheta_0.
\end{cases} \tag{37}$$

Lemma 4.2. *Label $s(\vartheta)=\xi_1(\vartheta)+i\xi_2(\vartheta)$ the root of (22) around $\theta=\theta_0$*

obeying $\xi_1(\vartheta_0) = 0, \xi_2(\vartheta_0) = \varrho_0$, *then* $Re\left[\frac{ds}{d\vartheta}\right]_{\vartheta=\vartheta_0,\varrho=\varrho_0} > 0$.

Proof Depending on (22), one gains

$$\left[2\alpha s^{2\alpha-1} + \alpha_1\alpha s^{\alpha-1}\right]\frac{ds}{d\vartheta} + \alpha_3\alpha s^{\alpha-1}e^{-s\vartheta}\frac{ds}{d\vartheta}$$

$$-e^{-s\vartheta}\left(\frac{ds}{d\vartheta}\vartheta + s\right)(\alpha_3 s^{\alpha} + \alpha_4) - 2\alpha_5 e^{-2s\vartheta}\left(\frac{ds}{d\vartheta}\vartheta + s\right) = 0. \tag{38}$$

By (38), one gets

$$\left(\frac{ds}{d\vartheta}\right)^{-1} = \frac{U}{M} - \frac{\vartheta}{s}, \tag{39}$$

where

$$\begin{cases} U = 2\alpha s^{2\alpha-1} + \alpha_1\alpha s^{\alpha-1} + \alpha_3\alpha s^{\alpha-1}e^{-s\vartheta}, \\ M = e^{-s\vartheta}s(\alpha_3 s^{\alpha} + \alpha_4) + 2\alpha_5\vartheta e^{-2s\vartheta}. \end{cases} \tag{40}$$

Then

$$\mathrm{Re}\left[\left(\frac{ds}{d\vartheta}\right)^{-1}\right] = \mathrm{Re}\left[\left(\frac{U}{M}\right)^{-1}\right]. \tag{41}$$

Hence

$$\mathrm{Re}\left[\left(\frac{ds}{d\vartheta}\right)^{-1}\right]_{\vartheta=\vartheta_0,\varrho=\varrho_0} = \frac{U_1M_1 + U_2M_2}{M_1^2 + M_2^2}. \tag{42}$$

Using (Q_3), one gains

$$\mathrm{Re}\left[\left(\frac{ds}{d\vartheta}\right)^{-1}\right]_{\vartheta=\vartheta_0,\varrho=\varrho_0} > 0. \tag{43}$$

The proof of Lemma 4.2 comes to an end. ■

Relying on the investigation above, the following result is lightly acquired.

Theorem 4.1. *If* (A_1)-(A_3) *are fulfilled, the positive equilibrium point* $E(v_{1*}, v_{2*})$ *of model (3) is locally asymptotically stable if* ϑ *remains in the range* $[0, \vartheta_0)$ *and model (3) is about to produce a Hopf bifurcation around* $E(v_{1*}, v_{2*})$ *when* ϑ *passes through the number* ϑ_0.

5 Control of bifurcation via delayed feedback controller

In this part, we are about to use PD$^\alpha$ controller to control the stability domain and Hopf bifurcation of model (3). The PD$^\alpha$ controller is designed as follows:

$$w_1(t) = \kappa[v_1(t) - v_1(t-\vartheta)], \tag{44}$$

where κ stand for the gain coefficient, ϑ denotes a delay. Adding (44) to the first equation of model (3), one gains

$$\begin{cases} \dfrac{d^\alpha v_1(t)}{dt^\alpha} = a - bv_1(t-\vartheta) - v_1(t)v_2^2(t) + \kappa[v_1(t) - v_1(t-\vartheta)], \\ \dfrac{d^\alpha v_2(t)}{dt^\alpha} = bv_1(t) + v_1(t)v_2^2(t) - v_2(t-\vartheta). \end{cases} \tag{45}$$

One can lightly know that model (45) owns the equilibrium point $E(v_{1*}, v_{2*})$. Linearizing model (45) around $E(v_{1*}, v_{2*})$ leads to

$$\begin{cases} \dfrac{d^\alpha \bar{v}_1(t)}{dt^\alpha} = -(v_{2*}^2 - \kappa)\bar{v}_1(t) - 2v_{1*}v_{2*}\bar{v}_2(t) - (b+\kappa)\bar{v}_1(t-\vartheta), \\ \dfrac{d^\alpha \bar{v}_2(t)}{dt^\alpha} = (b + v_{2*}^2)\bar{v}_1(t) + 2v_{1*}v_{2*}\bar{v}_2(t) - \bar{v}_2(t-\vartheta). \end{cases} \tag{46}$$

The characteristic equation of Eq. (46) is given by

$$\det \begin{bmatrix} s^\alpha + v_{2*}^2 - \kappa - (b+\kappa)e^{-s\vartheta} & 2v_{1*}v_{2*} \\ -(b+v_{2*}^2) & s^\alpha - 2v_{1*}v_{2*} + e^{-s\vartheta} \end{bmatrix} = 0, \tag{47}$$

which results in

$$s^{2\alpha} + \beta_1 s^\alpha + \beta_2 + (\beta_3 s^\alpha + \beta_4)e^{-s\vartheta} + \beta_5 e^{-2s\vartheta} = 0, \tag{48}$$

where

$$\begin{cases} \beta_1 = v_{2*}^2 - \kappa - 2v_{1*}v_{2*}, \\ \beta_2 = 2(b-\kappa)v_{1*}v_{2*}, \\ \beta_3 = 1 - (b+\kappa), \\ \beta_4 = 2(b+\kappa)v_{1*}v_{2*} + v_{2*}^2 - \kappa, \\ \beta_5 = -(b+\kappa). \end{cases} \tag{49}$$

The following essential hypothesis is provided:

$$(Q_4)\quad \beta_1+\beta_3>0, \beta_2+\beta_4+\beta_5>0.$$

Lemma 5.1. *Provided that* (Q_4) *holds, then the positive equilibrium point* $E(v_{1*}, v_{2*})$ *of model (45) is locally asymptotically stable.*

Proof If $\vartheta=0$, then Eq.(48) turns into:

$$\lambda^2+(\beta_1+\beta_3)\lambda+\beta_2+\beta_4+\beta_5=0. \tag{50}$$

In the light of (Q_4), the double roots λ_1 and λ_1 of (50) satify $|\arg(\lambda_1)|>\frac{\alpha\pi}{2}, |\arg(\lambda_2)|>\frac{\alpha\pi}{2}$. Exploiting Lemma 2.2, one can understand that the positive equilibrium point $E(v_{1*}, v_{2*})$ of model (45) is locally asymptotically stable. The proof comes to an end. ■

Now we rewrite Eq.(50) as

$$(s^{2\alpha}+\beta_1 s^{\alpha}+\beta_2)e^{s\alpha}+\beta_3 s^{\alpha}+\beta_4+\beta_5 e^{-s\alpha}=0. \tag{51}$$

Label $s=i\rho=\rho\left(\cos\frac{\pi}{2}+i\sin\frac{\pi}{2}\right)$ the root of Eq.(51). Then

$$\left[\rho^{2\alpha}(\cos\alpha\pi+i\sin\alpha\pi)+\beta_1\rho^{\alpha}\left(\cos\frac{\alpha\pi}{2}+i\sin\frac{\alpha\pi}{2}\right)+\beta_2\right]$$

$$\times(\cos\rho\vartheta+i\sin\rho\vartheta)+\beta_3\rho^{\alpha}\left(\cos\frac{\alpha\pi}{2}+i\sin\frac{\alpha\pi}{2}\right)$$

$$+\beta_4+\beta_5(\cos\rho\vartheta-i\sin\rho\vartheta)=0, \tag{52}$$

which results in

$$\begin{cases} e_1\cos\rho\vartheta-e_2\sin\rho\vartheta=e_3,\\ e_2\cos\rho\vartheta+e_1\sin\rho\vartheta=e_5, \end{cases} \tag{53}$$

where

$$\begin{cases} e_1=f_1\rho^{2\alpha}+f_2\rho^{\alpha}+f_3,\\ e_2=f_4\rho^{2\alpha}+f_5\rho^{\alpha},\\ e_3=f_6\rho^{\alpha}+f_7,\\ e_4=f_1\rho^{2\alpha}+f_2\rho^{\alpha}+f_8,\\ e_5=f_9\rho^{\alpha}, \end{cases} \tag{54}$$

where

$$\begin{cases} f_1 = \cos\alpha\pi, \\ f_2 = \beta_1 \cos\dfrac{\alpha\pi}{2}, \\ f_3 = \beta_2 + \beta_5, \\ f_4 = \sin\alpha\pi, \\ f_5 = \beta_1 \sin\dfrac{\alpha\pi}{2}, \\ f_6 = -\beta_3 \cos\dfrac{\alpha\pi}{2}, \\ f_7 = -\beta_4, \\ f_8 = \beta_2 - \beta_5, \\ f_9 = -\beta_3 \sin\dfrac{\alpha\pi}{2}. \end{cases} \tag{55}$$

In view of (53), we gain

$$\begin{cases} \cos\rho\vartheta = \dfrac{e_3e_4 + e_2e_5}{e_1e_4 + e_2^2}, \\ \sin\rho\vartheta = \dfrac{e_1e_5 - e_2e_3}{e_1e_4 + e_2^2} \end{cases} \tag{56}$$

and

$$(e_3e_4 + e_2e_5)^2 + (e_1e_5 - e_2e_3)^2 = (e_1e_4 + e_2^2)^2. \tag{57}$$

Using (57), one gains

$$\varepsilon_1\rho^{8\alpha} + \varepsilon_2\rho^{7\alpha} + \varepsilon_3\rho^{6\alpha} + \varepsilon_4\rho^{5\alpha} + \varepsilon_5\rho^{4\alpha} + \varepsilon_6\rho^{3\alpha} + \varepsilon_7\rho^{2\alpha} + \varepsilon_8\rho^{\alpha} + \varepsilon_9 = 0, \tag{58}$$

where

$$\begin{cases} \varepsilon_1 = (f_1^2 + f_4^2)^2, \\ \varepsilon_2 = 4(f_1^2 + f_4^2)^2(f_1f_2 + f_4f_5), \\ \varepsilon_3 = 4(f_1f_2 + f_4f_5)^2 + 2(f_1^2 + f_4^2) \\ \qquad \times (f_1f_8 + f_1f_3 + f_2^2 + f_5^2) \\ \qquad - (f_1f_6 + f_4f_6)^2 - (f_1f_9 - f_4f_6)^2, \\ \varepsilon_4 = 2(f_1^2 + f_4^2)(f_2f_8 + f_2f_3) \\ \qquad - 2(f_1f_6 + f_4f_6)(f_2f_6 + f_5f_6 + f_1f_7) \\ \qquad - 2(f_1f_9 - f_4f_6)(f_2f_9 - f_4f_7 - f_5f_6), \end{cases}$$

and

$$\begin{cases} \varepsilon_5 = (f_1f_8 + f_1f_3 + f_2^2 + f_5^2)^2 \\ \quad + 4(f_1f_2 + f_4f_5)(f_2f_8 + f_2f_3) \\ \quad - (f_2f_6 + f_5f_6 + f_1f_7)^2 \\ \quad - 2(f_1f_6 + f_4f_6)(f_6f_8 + f_2f_7) \\ \quad - (f_2f_9 - f_4f_7 - f_5f_6)^2 \\ \quad - 2(f_1f_9 - f_4f_6)(f_3f_9 - f_5f_7), \\ \varepsilon_6 = 4f_3f_8(f_1f_2 + f_4f_5) \\ \quad + 2(f_1f_8 + f_1f_3 + f_2^2 + f_5^2)(f_2f_8 + f_2f_3) \\ \quad - 2f_7f_8(f_1f_6 + f_4f_6) - 2(f_2f_6 + f_5f_6 + f_1f_7) \\ \quad \times (f_6f_8 + f_2f_7) - 2(f_2f_9 - f_4f_7 - f_5f_6) \\ \quad \times (f_3f_9 - f_5f_7), \\ \varepsilon_7 = 2f_3f_8(f_1f_8 + f_1f_3 + f_2^2 + f_5^2) \\ \quad + (f_2f_8 + f_2f_3)^2 - (f_6f_8 + f_2f_7)^2 \\ \quad - 2f_7f_8(f_2f_6 + f_5f_6 + f_1f_7) - (f_3f_9 - f_5f_7)^2, \\ \varepsilon_8 = 2f_3f_8(f_2f_8 + f_2f_3) - 2f_7f_8(f_6f_8 + f_2f_7), \\ \varepsilon_9 = (f_3f_8)^2 - (f_7f_8)^2. \end{cases} \tag{59}$$

Label

$$\Theta_2(\rho) = \varepsilon_1\rho^{8\alpha} + \varepsilon_2\rho^{7\alpha} + \varepsilon_3\rho^{6\alpha} + \varepsilon_4\rho^{5\alpha}$$

$$+\varepsilon_5\rho^{4\alpha} + \varepsilon_6\rho^{3\alpha} + \varepsilon_7\rho^{2\alpha} + \varepsilon_8\rho^{\alpha} + \varepsilon_9. \tag{60}$$

Suppose that

$$(Q_5)\ |f_3| < |f_7|$$

is fulfilled, consider that $\frac{d\Theta_2(\rho)}{d\rho} > 0, \forall\ \ \rho > 0$, then one easily know that Eq.(58) admits at the very least one positive real root. Hence Eq.(51) admits at the very least one couple of purely roots.

Suppose that Eq.(58) admits eight real roots (say $\varrho_j > 0 (j = 1, 2, \cdots, 8)$. In conformity with (56), one gains

$$\vartheta_i^k = \frac{1}{\varrho_i}\left[\arccos\frac{e_3e_4 + e_2e_5}{e_1e_4 + e_2^2} + 2k\pi\right], \tag{61}$$

where $k = 0, 1, 2, \cdots, i = 1, 2, \cdots, 8$. Label

$$\vartheta_* = \min_{i=1,2,\cdots,8}\{\vartheta_j^0\}, \rho_0 = \rho|_{\vartheta=\vartheta_*}. \tag{62}$$

Now we list the following indispensable hypothesis:

(Q_6) $S_1T_1 + S_2T_2 > 0$, where

$$\begin{cases} S_1 = 2\alpha\rho_0^{2\alpha-1}\cos\dfrac{(2\alpha-1)\pi}{2} + \beta_1\alpha\rho_0^{\alpha-1}\cos\dfrac{(\alpha-1)\pi}{2} \\ \quad + \beta_3\alpha\rho_0^{\alpha-1}\cos\dfrac{(\alpha-1)\pi}{2}\cos\rho_0\vartheta_* \\ \quad + \beta_3\alpha\rho_0^{\alpha-1}\sin\dfrac{(\alpha-1)\pi}{2}\sin\rho_0\vartheta_*, \\ S_2 = 2\alpha\rho_0^{2\alpha-1}\sin\dfrac{(2\alpha-1)\pi}{2} + \beta_1\alpha\rho_0^{\alpha-1}\sin\dfrac{(\alpha-1)\pi}{2} \\ \quad - \beta_3\alpha\rho_0^{\alpha-1}\cos\dfrac{(\alpha-1)\pi}{2}\sin\rho_0\vartheta_* \\ \quad + \beta_3\alpha\rho_0^{\alpha-1}\sin\dfrac{(\alpha-1)\pi}{2}\cos\rho_0\vartheta_*, \\ T_1 = \left(\beta_3\rho_0^{\alpha}\cos\dfrac{\alpha\pi}{2} + \beta_4\right)\rho_0\sin\rho_0\vartheta_* \\ \quad - \left(\beta_3\rho_0^{\alpha}\sin\dfrac{\alpha\pi}{2}\right)\rho_0\cos\rho_0\vartheta_*, \\ T_2 = \left(\beta_3\rho_0^{\alpha}\cos\dfrac{\alpha\pi}{2} + \alpha_4\right)\rho_0\cos\rho_0\vartheta_* \\ \quad + \left(\beta_3\rho_0^{\alpha}\sin\dfrac{\alpha\pi}{2}\right)\rho_0\sin\rho_0\vartheta_*. \end{cases} \tag{63}$$

Lemma 5.2. *Label $s(\vartheta) = \varsigma_1(\vartheta) + i\varsigma_2(\vartheta)$ the root of (48) around $\theta = \theta_*$ obeying $\varsigma_1(\vartheta_*) = 0, \varsigma_2(\vartheta_*) = \varrho_0$, then $Re\left[\frac{ds}{d\vartheta}\right]_{\vartheta=\vartheta_*,\rho=\rho_0} > 0$.*

Proof Relying on (48), one gains

$$\left[2\alpha s^{2\alpha-1} + \beta_1\alpha s^{\alpha-1}\right]\frac{ds}{d\vartheta} + \beta_3\alpha s^{\alpha-1}e^{-s\vartheta}\frac{ds}{d\vartheta}$$

$$-e^{-s\vartheta}\left(\frac{ds}{d\vartheta}\vartheta + s\right)(\beta_3 s^{\alpha} + \beta_4) - 2\beta_5 e^{-2s\vartheta}\left(\frac{ds}{d\vartheta}\vartheta + s\right) = 0. \tag{64}$$

By (64), one gets

$$\left(\frac{ds}{d\vartheta}\right)^{-1} = \frac{S}{T} - \frac{\vartheta}{s}, \tag{65}$$

where

$$\begin{cases} S = 2\alpha s^{2\alpha-1} + \beta_1 \alpha s^{\alpha-1} + \beta_3 \alpha s^{\alpha-1} e^{-s\vartheta}, \\ T = e^{-s\vartheta} s(\alpha_3 s^{\alpha} + \beta_4) + 2\beta_5 \vartheta e^{-2s\vartheta}. \end{cases} \tag{66}$$

Then

$$\mathrm{Re}\left[\left(\frac{ds}{d\vartheta}\right)^{-1}\right] = \mathrm{Re}\left[\left(\frac{S}{T}\right)^{-1}\right]. \tag{67}$$

Hence

$$\mathrm{Re}\left[\left(\frac{ds}{d\vartheta}\right)^{-1}\right]_{\vartheta=\vartheta_*,\rho=\rho_0} = \frac{S_1T_1 + S_2T_2}{T_1^2 + T_2^2}. \tag{68}$$

Using (Q_6), one gains

$$\mathrm{Re}\left[\left(\frac{ds}{d\vartheta}\right)^{-1}\right]_{\vartheta=\vartheta_*,\rho=\rho_0} > 0. \tag{69}$$

The proof of Lemma 5.2 comes to an end. ■

Relying on the investigation above, the following conclusion is lightly gained.

Theorem 5.1. *If (Q_4)-(Q_6) are fulfilled, the positive equilibrium point $E(v_{1*}, v_{2*})$ of model (45) is locally asymptotically stable if ϑ keeps in the range $[0, \vartheta_*)$ and model (45) will produces a Hopf bifurcation around $E(v_{1*}, v_{2*})$ when ϑ exceeds the number ϑ_*.*

6 Control of bifurcation via PD^{α} controller

In this part, we are about to design PD^{α} controller to control the stability domain and Hopf bifurcation of model (3). The PD^{α} controller is designed as follows:

$$w_2(t) = \sigma_p \left(v_2(t-\vartheta) - v_{2\star}\right) + \sigma_d \frac{d^{\alpha}\left(v_2(t) - v_{2\star}\right)}{dt^{\alpha}}, \tag{70}$$

where σ_p and $\sigma_d \neq 1$ denote the proportional control coefficient and the derivative control coefficient, respectively, ϑ is a delay. Adding (70) to the

second equation of model (3), one gains

$$\begin{cases} \dfrac{d^{\alpha}v_1(t)}{dt^{\alpha}} = a - bv_1(t-\vartheta) - v_1(t)v_2^2(t), \\ \dfrac{d^{\alpha}v_2(t)}{dt^{\alpha}} = bv_1(t) + v_1(t)v_2^2(t) - v_2(t-\vartheta) \\ \qquad\qquad + \sigma_p\left(v_2(t-\vartheta) - v_{2\star}\right) + \sigma_d \dfrac{d^{\alpha}\left(v_2(t) - v_{2\star}\right)}{dt^{\alpha}}. \end{cases} \tag{71}$$

Model (71) also takes the following expression:

$$\begin{cases} \dfrac{d^{\alpha}v_1(t)}{dt^{\alpha}} = a - bv_1(t-\vartheta) - v_1(t)v_2^2(t), \\ \dfrac{d^{\alpha}v_2(t)}{dt^{\alpha}} = \dfrac{1}{1-\sigma_d}\left[bv_1(t) + v_1(t)v_2^2(t) - v_2(t-\vartheta)\right. \\ \qquad\qquad \left. +\sigma_p\left(v_2(t-\vartheta) - v_{2*}\right)\right]. \end{cases} \tag{72}$$

Obviously, model (72) has the unique positive equilibrium point $E(v_{1*}, v_{2*})$. Linearizing model (72) at $E(v_{1*}, v_{2*})$ leads to

$$\begin{cases} \dfrac{d^{\alpha}\bar{v}_1(t)}{dt^{\alpha}} = -v_{2*}^2\bar{v}_1(t) - 2v_{1*}v_{2*}\bar{v}_2(t) - b\bar{v}_1(t-\vartheta), \\ \dfrac{d^{\alpha}\bar{v}_2(t)}{dt^{\alpha}} = \dfrac{b+v_{2*}^2}{1-\sigma_d}\bar{v}_1(t) + \dfrac{2v_{1*}v_{2*}}{1-\sigma_d}\bar{v}_2(t) - \dfrac{1-\sigma_p}{1-\sigma_d}\bar{v}_2(t-\vartheta). \end{cases} \tag{73}$$

The characteristic equation of Eq. (73) is given by

$$\det\begin{bmatrix} s^{\alpha} + v_{2*}^2 - be^{-s\vartheta} & 2v_{1*}v_{2*} \\ -\frac{b+v_{2*}^2}{1-\sigma_d} & s^{\alpha} - \frac{2v_{1*}v_{2*}}{1-\sigma_d} + \frac{1-\sigma_p}{1-\sigma_d}e^{-s\vartheta} \end{bmatrix} = 0, \tag{74}$$

which results in

$$s^{2\alpha} + \gamma_1 s^{\alpha} + \gamma_2 + (\gamma_3 s^{\alpha} + \gamma_4)e^{-s\vartheta} + \gamma_5 e^{-2s\alpha} = 0, \tag{75}$$

where

$$\begin{cases} \gamma_1 = v_{2*}^2 - \dfrac{2v_{1*}v_{2*}}{1-\sigma_d}, \\ \gamma_2 = \dfrac{2v_{1*}v_{2*}(b+v_{2*}^2) - v_{2*}^2(2v_{1*}v_{2*})}{1-\sigma_d}, \\ \gamma_3 = \dfrac{1-\sigma_p}{1-\sigma_d} - b, \\ \gamma_4 = \dfrac{2v_{1*}v_{2*}b}{1-\sigma_d} + \dfrac{v_{2*}^2(1-\sigma_p)}{1-\sigma_d}, \\ \gamma_5 = -\dfrac{b(1-\sigma_p)}{1-\sigma_d}. \end{cases} \tag{76}$$

The following essential hypothesis is provided:

$$(Q_7) \quad \gamma_1 + \gamma_3 > 0, \gamma_2 + \gamma_4 + \gamma_5 > 0.$$

Lemma 6.1. *Provided that* (Q_7) *holds, then the positive equilibrium point* $E(v_{1*}, v_{2*})$ *of model (71) is locally asymptotically stable.*

Proof If $\vartheta = 0$, then Eq.(75) turns into:

$$\lambda^2 + (\gamma_1 + \gamma_3)\lambda + \gamma_2 + \gamma_4 + \gamma_5 = 0. \tag{77}$$

In the light of (Q_7), the double roots λ_1 and λ_1 of (77) satisfy $|\arg(\lambda_1)| > \frac{\alpha\pi}{2}, |\arg(\lambda_2)| > \frac{\alpha\pi}{2}$. Exploiting Lemma 2.2, one can understand that the positive equilibrium point $E(v_{1*}, v_{2*})$ of model (71) is locally asymptotically stable. The proof comes to an end. ■

Now we rewrite Eq.(75) as

$$(s^{2\alpha} + \gamma_1 s^\alpha + \gamma_2)e^{s\alpha} + \gamma_3 s^\alpha + \gamma_4 + \gamma_5 e^{-s\vartheta} = 0. \tag{78}$$

Label $s = i\phi = \phi\left(\cos\frac{\pi}{2} + i\sin\frac{\pi}{2}\right)$ the root of Eq.(78). Then

$$\begin{aligned} &\left[\phi^{2\alpha}(\cos\alpha\pi + i\sin\alpha\pi) + \gamma_1\phi^\alpha\left(\cos\frac{\alpha\pi}{2} + i\sin\frac{\alpha\pi}{2}\right) + \gamma_2\right] \\ &\times(\cos\phi\vartheta + i\sin\phi\vartheta) + \gamma_3\phi^\alpha\left(\cos\frac{\alpha\pi}{2} + i\sin\frac{\alpha\pi}{2}\right) \\ &+\gamma_4 + \gamma_5(\cos\phi\vartheta - i\sin\phi\vartheta) = 0, \end{aligned} \tag{79}$$

which results in

$$\begin{cases} g_1 \cos\phi\vartheta - g_2 \sin\phi\vartheta = g_3, \\ g_2 \cos\phi\vartheta + g_4 \sin\phi\vartheta = g_5, \end{cases} \tag{80}$$

where

$$\begin{cases} g_1 = h_1\phi^{2\alpha} + h_2\phi^{\alpha} + h_3, \\ g_2 = h_4\phi^{2\alpha} + h_5\phi^{\alpha}, \\ g_3 = h_6\phi^{\alpha} + h_7, \\ g_4 = h_1\phi^{2\alpha} + h_2\phi^{\alpha} + h_8, \\ g_5 = h_9\phi^{\alpha}, \end{cases} \tag{81}$$

where

$$\begin{cases} h_1 = \cos\alpha\pi, \\ h_2 = \gamma_1 \cos\dfrac{\alpha\pi}{2}, \\ h_3 = \gamma_2 + \gamma_5, \\ h_4 = \sin\alpha\pi, \\ h_5 = \gamma_1 \sin\dfrac{\alpha\pi}{2}, \\ h_6 = -\gamma_3 \cos\dfrac{\alpha\pi}{2}, \\ h_7 = -\gamma_4, \\ h_8 = \gamma_2 - \gamma_5, \\ h_9 = -\gamma_3 \sin\dfrac{\alpha\pi}{2}. \end{cases} \tag{82}$$

In view of (80), we gain

$$\begin{cases} \cos\phi\vartheta = \dfrac{g_3g_4 + g_2g_5}{g_1g_4 + g_2^2}, \\ \sin\phi\vartheta = \dfrac{g_1g_5 - g_2g_3}{g_1g_4 + g_2^2} \end{cases} \tag{83}$$

and

$$(g_3g_4 + g_2g_5)^2 + (g_1g_5 - g_2g_3)^2 = (g_1g_4 + g_2^2)^2. \tag{84}$$

Using (84), one gains

$$l_1\phi^{8\alpha} + l_2\phi^{7\alpha} + l_3\phi^{6\alpha} + l_4\phi^{5\alpha} + l_5\phi^{4\alpha} + l_6\phi^{3\alpha} + l_7\phi^{2\alpha} + l_8\phi^{\alpha} + l_9 = 0, \tag{85}$$

where

$$\begin{cases} l_1 = (h_1^2 + h_4^2)^2, \\ l_2 = 4(h_1^2 + h_4^2)^2(h_1h_2 + h_4h_5), \\ l_3 = 4(h_1h_2 + h_4h_5)^2 + 2(h_1^2 + h_4^2)(h_1h_8 + h_1h_3 + h_2^2 + h_5^2) \\ \quad - (h_1h_6 + h_4h_6)^2 - (h_1h_9 - h_4h_6)^2, \\ l_4 = 2(h_1^2 + h_4^2)(h_2h_8 + h_2h_3) \\ \quad - 2(h_1h_6 + h_4h_6)(h_2h_6 + h_5h_6 + h_1h_7) \\ \quad - 2(h_1h_9 - h_4h_6)(h_2h_9 - h_4h_7 - h_5h_6), \\ l_5 = (h_1h_8 + h_1h_3 + h_2^2 + h_5^2)^2 + 4(h_1h_2 + h_4h_5)(h_2h_8 + h_2h_3), \\ \quad - (h_2h_6 + h_5h_6 + h_1h_7)^2 - 2(h_1h_6 + h_4h_6)(h_6h_8 + h_2h_7) \\ \quad - (h_2h_9 - h_4h_7 - h_5h_6)^2 - 2(h_1h_9 - h_4h_6)(h_3h_9 - h_5h_7), \\ l_6 = 4h_3h_8(h_1h_2 + h_4h_5) + 2(h_1h_8 + h_1h_3 + h_2^2 + h_5^2) \\ \quad \times (h_2h_8 + h_2h_3) - 2h_7h_8(h_1h_6 + h_4h_6) \\ \quad - 2(h_2h_6 + h_5h_6 + h_1h_7)(h_6h_8 + h_2h_7) \\ \quad - 2(h_2h_9 - h_4h_7 - h_5h_6)(h_3h_9 - h_5h_7), \\ l_7 = 2h_3h_8(h_1h_8 + h_1h_3 + h_2^2 + h_5^2) + (h_2h_8 + h_2h_3)^2 \\ \quad - (h_6h_8 + h_2h_7)^2 - 2h_7h_8(h_2h_6 + h_5h_6 + h_1h_7) \\ \quad - (h_3h_9 - h_5h_7)^2, \\ l_8 = 2h_3h_8(h_2h_8 + h_2h_3) - 2h_7h_8(h_6h_8 + h_2h_7), \\ l_9 = (h_3h_8)^2 - (h_7h_8)^2. \end{cases} \tag{86}$$

Label

$$\Theta_3(\phi) = l_1\phi^{8\alpha} + l_2\phi^{7\alpha} + l_3\phi^{6\alpha} + l_4\phi^{5\alpha} + l_5\phi^{4\alpha} + l_6\phi^{3\alpha} + l_7\phi^{2\alpha} + l_8\phi^{\alpha} + l_9. \tag{87}$$

Suppose that

$$(Q_8)\ |h_3| < |h_7|$$

is fulfilled, consider that $\frac{d\Theta_3(\phi)}{d\phi} > 0, \forall\ \ \phi > 0$, then one easily know that Eq.(85) admits at the very least one positive real root. Hence Eq.(78) admits at the very least one couple of purely roots.

Suppose that Eq.(85) admits eight real roots (say $\phi_i > 0 (i = 1, 2, \cdots, 8)$.

In conformity with (83), one gains

$$\vartheta_i^k = \frac{1}{\varrho_i}\left[\arccos\left(\frac{g_3g_4+g_2g_5}{g_1g_4+g_2^2}\right)+2k\pi\right], \tag{88}$$

where $k=0,1,2,\cdots,i=1,2,\cdots,8$. Label

$$\vartheta_\star = \min_{i=1,2,\cdots,8}\{\vartheta_i^0\}, \phi_0 = \phi|_{\vartheta=\vartheta_\star}. \tag{89}$$

Now we list the following indispensable hypothesis:

(Q_9) $V_1Z_1+V_2Z_2>0$, where

$$\begin{cases} V_1 = 2\alpha\phi_0^{2\alpha-1}\cos\dfrac{(2\alpha-1)\pi}{2}+\gamma_1\alpha\phi_0^{\alpha-1}\cos\dfrac{(\alpha-1)\pi}{2} \\ \quad +\gamma_3\alpha\phi_0^{\alpha-1}\cos\dfrac{(\alpha-1)\pi}{2}\cos\varrho_0\vartheta_0 \\ \quad +\gamma_3\alpha\phi_0^{\alpha-1}\sin\dfrac{(\alpha-1)\pi}{2}\sin\phi_0\vartheta_\star, \\ V_2 = 2\alpha\phi_0^{2\alpha-1}\sin\dfrac{(2\alpha-1)\pi}{2}+\gamma_1\alpha\phi_0^{\alpha-1}\sin\dfrac{(\alpha-1)\pi}{2} \\ \quad -\gamma_3\alpha\phi_0^{\alpha-1}\cos\dfrac{(\alpha-1)\pi}{2}\sin\phi_0\vartheta_\star \\ \quad +\gamma_3\alpha\phi_0^{\alpha-1}\sin\dfrac{(\alpha-1)\pi}{2}\cos\phi_0\vartheta_\star, \\ Z_1 = \left(\gamma_3\phi_0^\alpha\cos\dfrac{\alpha\pi}{2}+\gamma_4\right)\phi_0\sin\phi_0\vartheta_\star \\ \quad -\left(\gamma_3\phi_0^\alpha\sin\dfrac{\alpha\pi}{2}\right)\phi_0\cos\phi_0\vartheta_\star, \\ Z_2 = \left(\gamma_3\phi_0^\alpha\cos\dfrac{\alpha\pi}{2}+\gamma_4\right)\phi_0\cos\phi_0\vartheta_\star \\ \quad +\left(\gamma_3\phi_0^\alpha\sin\dfrac{\alpha\pi}{2}\right)\phi_0\sin\phi_0\vartheta_\star. \end{cases} \tag{90}$$

Lemma 6.2. *Label $s(\vartheta)=\zeta_1(\vartheta)+i\zeta_2(\vartheta)$ the root of (75) around $\theta=\theta_\star$ obeying $\zeta_1(\vartheta_\star)=0,\zeta_2(\vartheta_\star)=\phi_0$, then $Re\left[\frac{ds}{d\vartheta}\right]_{\vartheta=\vartheta_\star,\phi=\phi_0}>0$.*

Proof Relying on (75), one gains

$$\left[2\alpha s^{2\alpha-1}+\gamma_1\alpha s^{\alpha-1}\right]\frac{ds}{d\vartheta}+\gamma_3\alpha s^{\alpha-1}e^{-s\vartheta}\frac{ds}{d\vartheta}$$

$$-e^{-s\vartheta}\left(\frac{ds}{d\vartheta}\vartheta+s\right)(\gamma_3s^\alpha+\gamma_4)-2\gamma_5e^{-2s\vartheta}\left(\frac{ds}{d\vartheta}\vartheta+s\right)=0. \tag{91}$$

By (91), one gets

$$\left(\frac{ds}{d\vartheta}\right)^{-1} = \frac{V}{Z} - \frac{\vartheta}{s}, \tag{92}$$

where

$$\begin{cases} V = 2\alpha s^{2\alpha-1} + \gamma_1 \alpha s^{\alpha-1} + \gamma_3 \alpha s^{\alpha-1} e^{-s\vartheta}, \\ Z = e^{-s\vartheta} s(\gamma_3 s^{\alpha} + \gamma_4) + 2\gamma_5 \vartheta e^{-2s\vartheta}. \end{cases} \tag{93}$$

Then

$$\mathrm{Re}\left[\left(\frac{ds}{d\vartheta}\right)^{-1}\right] = \mathrm{Re}\left[\left(\frac{V}{Z}\right)^{-1}\right]. \tag{94}$$

Hence

$$\mathrm{Re}\left[\left(\frac{ds}{d\vartheta}\right)^{-1}\right]_{\vartheta=\vartheta_\star,\phi=\phi_0} = \frac{V_1 Z_1 + V_2 Z_2}{Z_1^2 + Z_2^2}. \tag{95}$$

Using (Q_9), one gains

$$\mathrm{Re}\left[\left(\frac{ds}{d\vartheta}\right)^{-1}\right]_{\vartheta=\vartheta_\star,\phi=\phi_0} > 0. \tag{96}$$

The proof of Lemma 6.2 comes to an end. ■

Relying on the exploration above, the following conclusion can be lightly gained.

Theorem 6.1. *If (Q_7)-(Q_9) are fulfilled, the positive equilibrium point $E(v_{1*}, v_{2*})$ of model (3) is locally asymptotically stable if ϑ keeps in the range $[0, \vartheta_\star)$ and model (3) is about to generate a Hopf bifurcation around $E(v_{1*}, v_{2*})$ when ϑ exceeds the number $\vartheta_\star$.*

7 Computer simulations

In this part, we are about to perform computer simulation to check the correctness of Theorem 4.1, Theorem 5.1 and Theorem 6.1 by computer. We provide the three examples as follows.

Example 7.1. Give the following fractional-order delayed glycolytic os-

cillator model:

$$\begin{cases} \dfrac{d^{0.98}v_1(t)}{dt^{0.98}} = 0.5 - 0.6v_1(t-\vartheta) - v_1(t)v_2^2(t), \\ \dfrac{d^{0.98}v_2(t)}{dt^{0.98}} = 0.6v_1(t) + v_1(t)v_2^2(t) - v_2(t-\vartheta). \end{cases} \tag{97}$$

It is obvious that model (97) admits the unique equilibrium point $E(0.59, 0.5)$. Exploiting computer software, we can lightly gain $\varrho_0 = 5.3341$ and $\vartheta_0 = 0.85$. The three conditions (Q_1)-(Q_3) for Theorem 4.1 are met. To check the correctness of the assertion of Theorem 4.1, we consider two unequal delay values. Label $\vartheta = 0.83 < \vartheta_0 = 0.85$. Then the numerical simulation results of model (97) are presented in Figures 1-4. In the light of Figures 1-4, we can lightly understand that the equilibrium point $E(0.59, 0.5)$ of model (97) maintains locally asymptotically stable status. Figure 1 demonstrates that the variable $v_1 \to 0.59$ as $t \to \infty$;

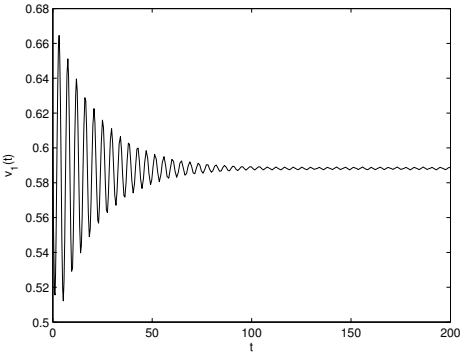

Figure 1. The trajectory of model (97) concerning $\vartheta = 0.83 < \vartheta_0 = 0.85$. The equilibrium point $E(0.59, 0.5)$ of model (97) remains locally asymptotically stable state. The variable $v_1 \to 0.59$ as $t \to \infty$.

Figure 2 demonstrates that the variable $v_2 \to 0.5$ as $t \to \infty$;

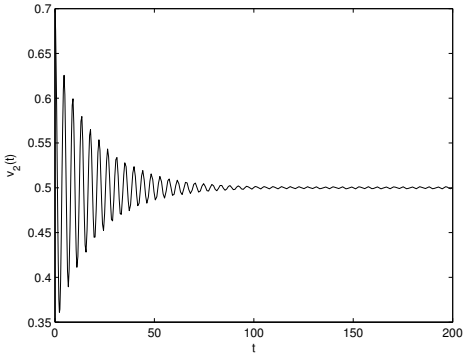

Figure 2. The trajectory of model (97) concerning $\vartheta = 0.83 < \vartheta_0 = 0.85$. The equilibrium point $E(0.59, 0.5)$ of model (97) remains locally asymptotically stable state. The variable $v_2 \to 0.5$ as $t \to \infty$.

Figure 3 reveals the intercorrelations between variables v_1 and v_2 as $t \to \infty$;

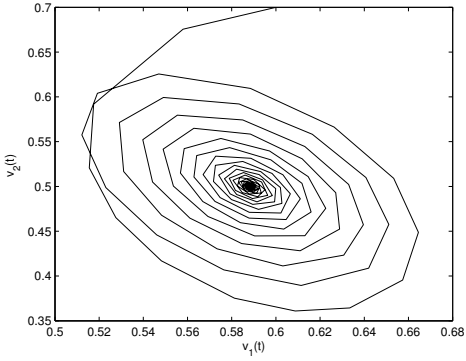

Figure 3. The phase diagram of model (97) concerning $\vartheta = 0.83 < \vartheta_0 = 0.85$. The equilibrium point $E(0.59, 0.5)$ of model (97) remains locally asymptotically stable state. The variable $v_1 \to 0.59$ and the variable $v_2 \to 0.5$ as $t \to \infty$.

Figure 4 demonstrates the intercorrelations among variables v_1 and v_2 and the time t. Label $\vartheta = 0.88 > \vartheta_0 = 0.85$.

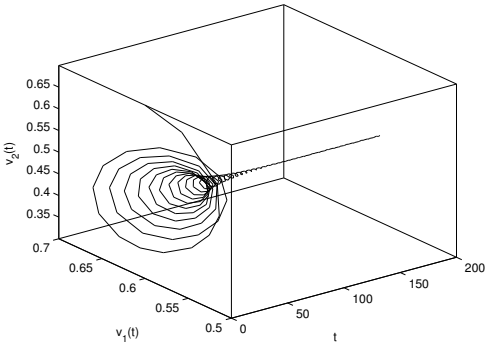

Figure 4. The three-dimensional space of model (97) concerning $\vartheta = 0.83 < \vartheta_0 = 0.85$. The equilibrium point $E(0.59, 0.5)$ of model (97) remains locally asymptotically stable state. It shows the intercorrelations among variables v_1, v_2 and the time t.

Then the numerical simulation results of model (97) are presented in Figures 5-8. In the light of Figures 5-8, we can lightly understand that a family of limit cycles (Hopf bifurcations) are about to appear around the $E(0.59, 0.5)$. Figure 5 demonstrates that the variable v_1 is about to preserve periodic vibration state around the number 0.59 as $t \to \infty$;

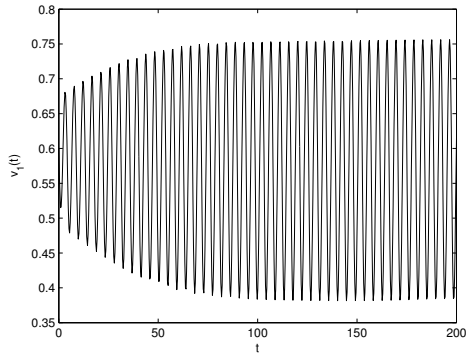

Figure 5. The trajectory of model (97) concerning $\vartheta = 0.88 > \vartheta_0 = 0.85$. A family of limit cycles (Hopf bifurcations) appear around $E(0.59, 0.5)$. The variable v_1 is about to produce periodic vibration around the number 0.59 as $t \to \infty$.

Figure 6 demonstrates that the variable v_2 is about to preserve periodic vibration state around the number 0.5 as $t \to \infty$;

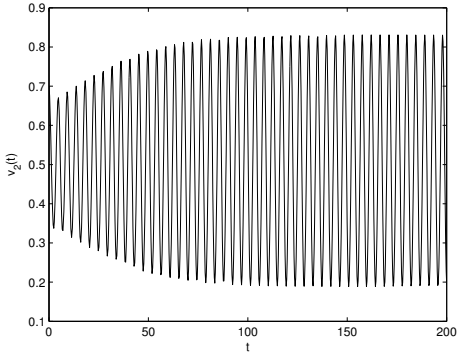

Figure 6. The trajectory of model (97) concerning $\vartheta = 0.88 > \vartheta_0 = 0.85$. A family of limit cycles (Hopf bifurcations) appear around $E(0.59, 0.5)$. The variable v_2 is about to produce periodic vibration around the number 0.5 as $t \to \infty$.

Figure 7 demonstrates the intercorrelations between the variables v_1 and v_2 as $t \to \infty$;

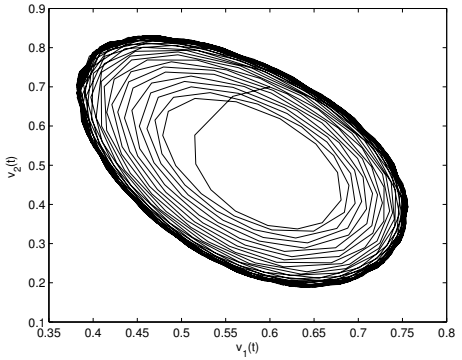

Figure 7. The phase diagram of model (97) concerning $\vartheta = 0.88 > \vartheta_0 = 0.85$. A family of limit cycles (Hopf bifurcations) appear around $E(0.59, 0.5)$. The variables v_1 and v_2 is about to produce periodic vibration around the numbers 0.59 and 0.5, respectively.

Figure 8 demonstrates the intercorrelations among the variables v_1, v_2

and the time t.

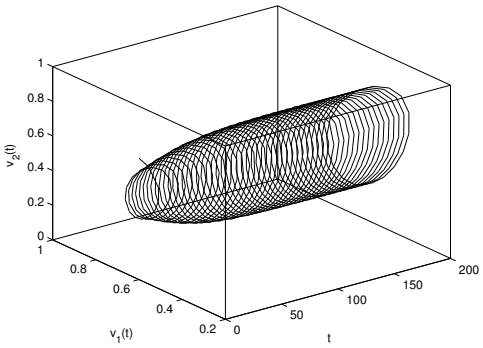

Figure 8. The three-dimensional space of model (97) concerning $\vartheta = 0.88 > \vartheta_0 = 0.85$. A family of limit cycles (Hopf bifurcations) appear around $E(0.59, 0.5)$. The variables v_1 and v_2 is about to produce periodic vibration around the numbers 0.59 and 0.5, respectively. It shows the intercorrelations among variables v_1, v_2 and the time t.

The bifurcation figures of model (97) are also presented in Figures 9-10.

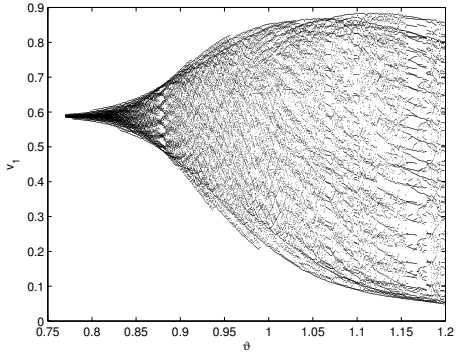

Figure 9. The bifurcation graph of model (97): ϑ versus v_1. It shows that the bifurcation value $\vartheta_0 \approx 0.85$.

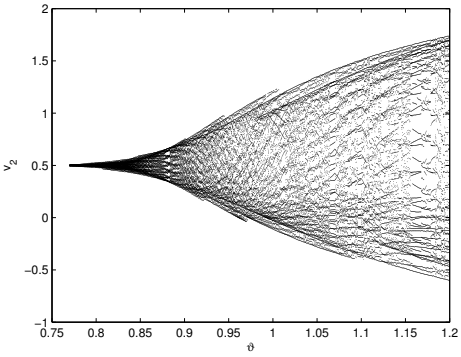

Figure 10. The bifurcation graph of model (97): ϑ versus v_2. It shows that the bifurcation value $\vartheta_0 \approx 0.85$.

Example 7.2. Give the following fractional-order controlled glycolysis model with delay:

$$\begin{cases} \dfrac{d^{0.98}v_1(t)}{dt^{0.98}} = 0.5 - 0.6v_1(t-\vartheta) - v_1(t)v_2^2(t) + 0.5[v_1(t) - v_1(t-\vartheta)], \\ \dfrac{d^{0.98}v_2(t)}{dt^{0.98}} = 0.6v_1(t) + v_1(t)v_2^2(t) - v_2(t-\vartheta). \end{cases} \tag{98}$$

It is obvious that model (98) admits the unique equilibrium point $E(0.59, 0.5)$. Exploiting computer software, we can lightly gain $\rho_0 = 2.0093$ and $\vartheta_\star = 0.7$. The three conditions (Q_4)-(Q_6) for Theorem 5.1 are met. To check the correctness of the assertion of Theorem 5.1, we consider two unequal delay values. Label $\vartheta = 0.66 < \vartheta_* = 0.7$. Then the numerical simulation results of model (98) are presented in Figures 11-14. In the light of Figures 11-14, we can lightly understand that the equilibrium point $E(0.59, 0.5)$ of model (98) maintains locally asymptotically stable status. Figure 11 demonstrates that the variable $v_1 \to 0.59$ as $t \to \infty$; Figure 12 demonstrates that the variable $v_2 \to 0.5$ as $t \to \infty$; Figure 13 reveals the intercorrelations between variables v_1 and v_2 as $t \to \infty$; Figure 14 demonstrates the intercorrelations among variables v_1 and v_2 and the time t. Label $\vartheta = 0.8 > \vartheta_* = 0.7$.

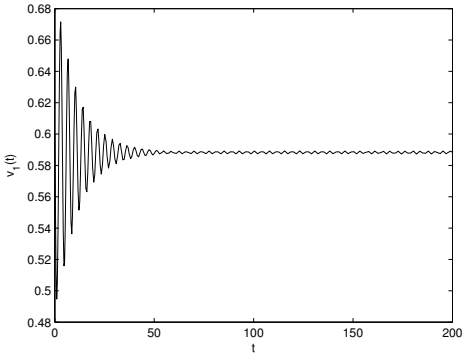

Figure 11. The trajectory of model (98) concerning $\vartheta = 0.66 < \vartheta_* = 0.7$. The equilibrium point $E(0.59, 0.5)$ of model (98) remains locally asymptotically stable state. The variable $v_1 \to 0.59$ as $t \to \infty$.

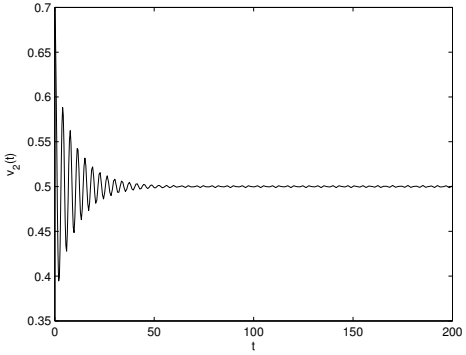

Figure 12. The trajectory of model (98) concerning $\vartheta = 0.66 < \vartheta_* = 0.7$. The equilibrium point $E(0.59, 0.5)$ of model (98) remains locally asymptotically stable state. The variable $v_2 \to 0.5$ as $t \to \infty$.

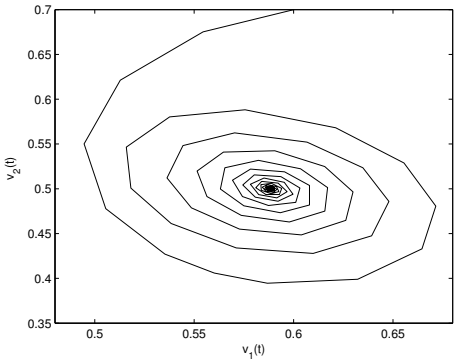

Figure 13. The phase diagram of model (98) concerning $\vartheta = 0.66 < \vartheta_* = 0.7$. The equilibrium point $E(0.59, 0.5)$ of model (98) remains locally asymptotically stable state. The variable $v_1 \to 0.59$ and the variable $v_2 \to 0.5$ as $t \to \infty$.

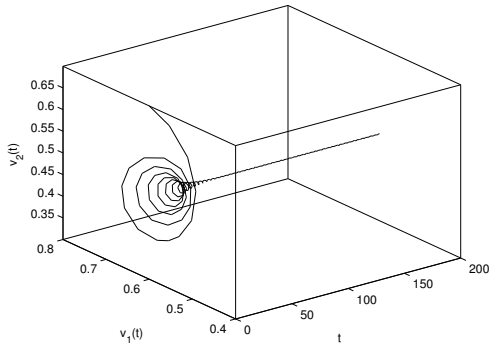

Figure 14. The three-dimensional space of model (98) concerning $\vartheta = 0.66 < \vartheta_* = 0.7$. The equilibrium point $E(0.59, 0.5)$ of model (98) remains locally asymptotically stable state. It shows the intercorrelations among variables v_1, v_2 and the time t.

Then the numerical simulation results of model (98) are presented in Figures 15-18. In the light of Figures 15-18, we can lightly understand that a family of limit cycles (Hopf bifurcations) are about to appear around the $E(0.59, 0.5)$. Figure 15 demonstrates that the variable v_1 is about to preserve periodic vibration state around the number 0.59 as $t \to \infty$;

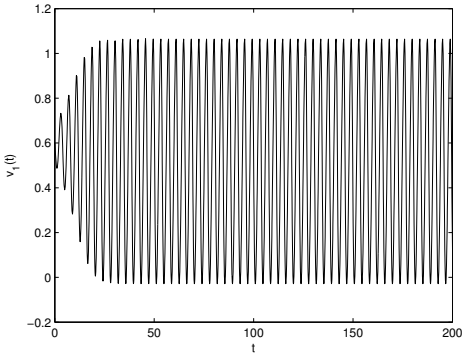

Figure 15. The trajectory of model (98) concerning $\vartheta = 0.8 > \vartheta_* = 0.7$. A family of limit cycles (Hopf bifurcations) appear around $E(0.59, 0.5)$. The variable v_1 is about to produce periodic vibration around the number 0.59 as $t \to \infty$.

Figure 16 demonstrates that the variable v_2 is about to preserve periodic vibration state around the number 0.5 as $t \to \infty$;

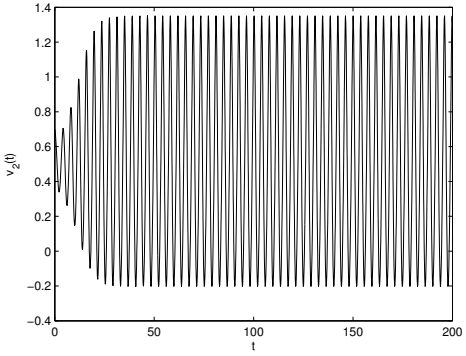

Figure 16. The trajectory of model (98) concerning $\vartheta = 0.8 > \vartheta_* = 0.7$. A family of limit cycles (Hopf bifurcations) appear around $E(0.59, 0.5)$. The variable v_2 is about to produce periodic vibration around the number 0.59 as $t \to \infty$.

Figure 17 demonstrates the intercorrelations between the variables v_1 and v_2 as $t \to \infty$;

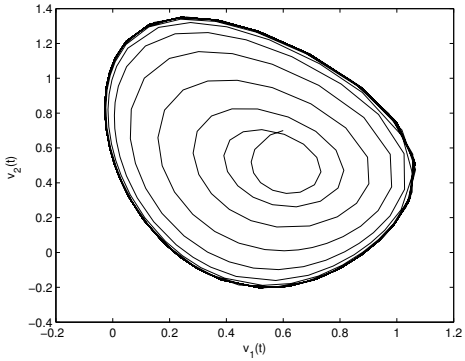

Figure 17. The phase diagram of model (98) concerning $\vartheta = 0.8 > \vartheta_* = 0.7$. A family of limit cycles (Hopf bifurcations) appear around $E(0.59, 0.5)$. The variables v_1 and v_2 is about to produce periodic vibration around the numbers 0.59 and 0.5, respectively.

Figure 18 demonstrates the intercorrelations among the variables v_1, v_2 and the time t.

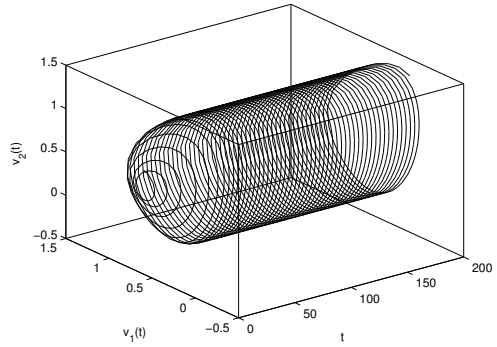

Figure 18. The three-dimensional space of model (98) concerning $\vartheta = 0.8 > \vartheta_* = 0.7$. A family of limit cycles (Hopf bifurcations) appear around $E(0.59, 0.5)$. The variables v_1 and v_2 is about to produce periodic vibration around the numbers 0.59 and 0.5, respectively. It shows the intercorrelations among variables v_1, v_2 and the time t.

The bifurcation figures of model (98) are also presented in Figures 19-20.

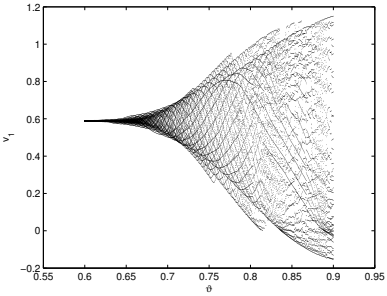

Figure 19. The bifurcation graph of model (98): ϑ versus v_1. It shows that the bifurcation value $\vartheta_0 \approx 0.7$.

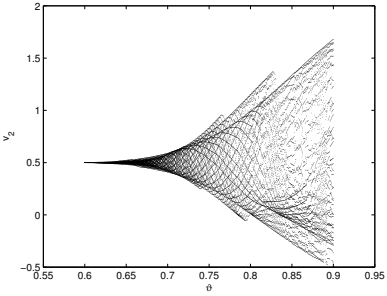

Figure 20. The bifurcation graph of model (98): ϑ versus v_2. It shows that the bifurcation value $\vartheta_0 \approx 0.7$.

Example 7.3. Give the following fractional-order controlled glycolysis model with delay:

$$\begin{cases} \dfrac{d^{0.98}v_1(t)}{dt^{0.98}} = 0.5 - 0.6v_1(t-\vartheta) - v_1(t)v_2^2(t), \\ \dfrac{d^{0.98}v_2(t)}{dt^{0.98}} = 0.6v_1(t) + v_1(t)v_2^2(t) - v_2(t-\vartheta) \\ \qquad\qquad + 0.3\,(v_2(t-\vartheta) - v_{2\star}) + 0.5\dfrac{d^{0.98}\,(v_2(t) - v_{2\star})}{dt^{0.98}}. \end{cases} \tag{99}$$

It is obvious that model (99) admits the unique equilibrium point $E(0.59, 0.5)$. Exploiting computer software, we can lightly gain $\phi_0 = 2.7723$ and $\vartheta_\star = 0.59$. The three conditions (Q_7)-(Q_9) for Theorem 5.1 are met. To check the correctness of the assertion of Theorem 5.1, we consider two

unequal delay values. Label $\vartheta = 0.57 < \vartheta_\star = 0.59$. Then the numerical simulation results of model (99) are presented in Figures 21-24. In the light of Figures 21-24, we can lightly understand that the equilibrium point $E(0.59, 0.5)$ of model (99) maintains locally asymptotically stable status. Figure 21 demonstrates that the variable $v_1 \to 0.59$ as $t \to \infty$;

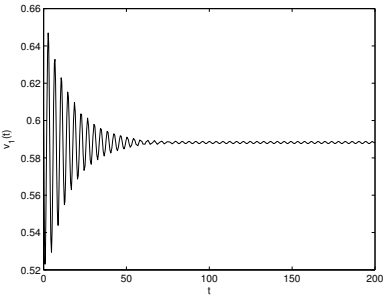

Figure 21. The trajectory of model (99) concerning $\vartheta = 0.57 < \vartheta_\star = 0.59$. The equilibrium point $E(0.59, 0.5)$ of model (99) remains locally asymptotically stable state. The variable $v_1 \to 0.59$ as $t \to \infty$.

Figure 22 demonstrates that the variable $v_2 \to 0.5$ as $t \to \infty$;

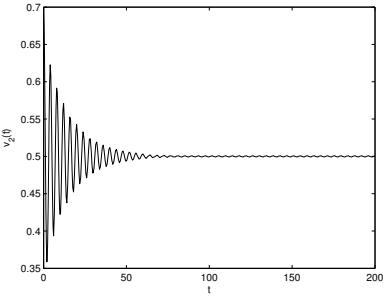

Figure 22. The trajectory of model (99) concerning $\vartheta = 0.57 < \vartheta_\star = 0.59$. The equilibrium point $E(0.59, 0.5)$ of model (99) remains locally asymptotically stable state. The variable $v_2 \to 0.5$ as $t \to \infty$.

Figure 23 reveals the intercorrelations between variables v_1 and v_2 as $t \to \infty$;

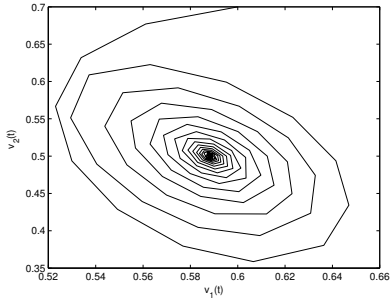

Figure 23. The phase diagram of model (99) concerning $\vartheta = 0.57 < \vartheta_\star = 0.59$. The equilibrium point $E(0.59, 0.5)$ of model (99) remains locally asymptotically stable state. The variable $v_1 \to 0.59$ and the variable $v_2 \to 0.5$ as $t \to \infty$.

Figure 24 demonstrates the intercorrelations among variables v_1 and v_2 and the time t.

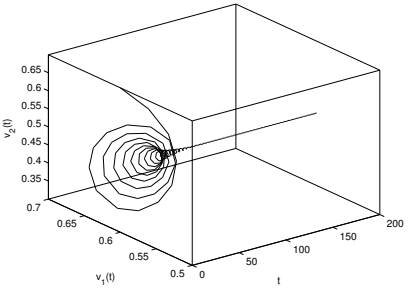

Figure 24. The three-dimensional space of model (99) concerning $\vartheta = 0.57 < \vartheta_\star = 0.59$. The equilibrium point $E(0.59, 0.5)$ of model (99) remains locally asymptotically stable state. It shows the intercorrelations among variables v_1, v_2 and the time t.

Label $\vartheta = 0.65 > \vartheta_\star = 0.59$. Then the numerical simulation results of model (99) are presented in Figures 25-28. In the light of Figures 5-8, we can lightly understand that a family of limit cycles (Hopf bifurcations) are about to appear around the $E(0.59, 0.5)$. Figure 25 demonstrates that the variable v_1 is about to preserve periodic vibration state around the number 0.59 as $t \to \infty$;

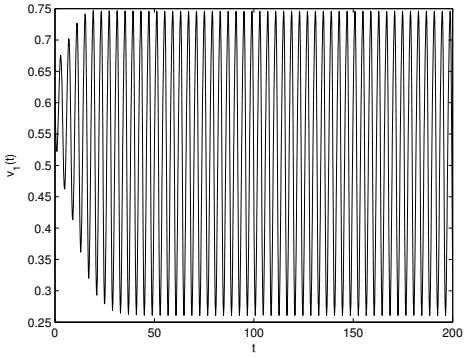

Figure 25. The trajectory of model (99) concerning $\vartheta = 0.65 > \vartheta_\star = 0.59$. A family of limit cycles (Hopf bifurcations) appear around $E(0.59, 0.5)$. The variable v_1 is about to produce periodic vibration around the number 0.59 as $t \to \infty$.

Figure 26 demonstrates that the variable v_2 is about to preserve periodic vibration state around the number 0.5 as $t \to \infty$;

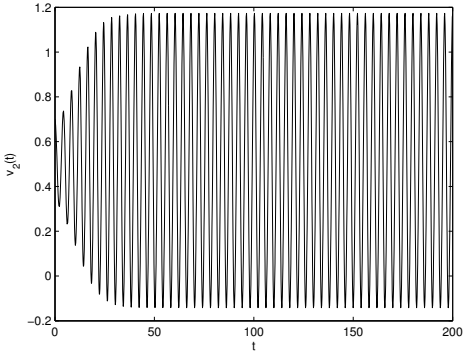

Figure 26. The trajectory of model (99) concerning $\vartheta = 0.65 > \vartheta_\star = 0.59$. A family of limit cycles (Hopf bifurcations) appear around $E(0.59, 0.5)$. The variable v_2 is about to produce periodic vibration around the number 0.5 as $t \to \infty$.

Figure 27 demonstrates the intercorrelations between the variables v_1 and v_2 as $t \to \infty$;

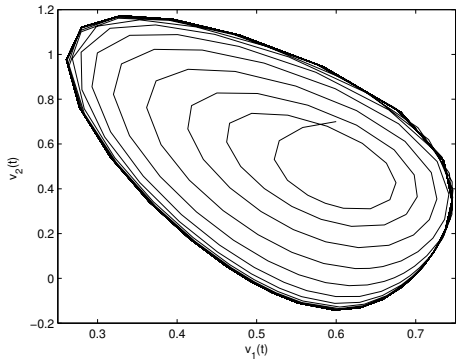

Figure 27. The phase diagram of model (99) concerning $\vartheta = 0.65 > \vartheta_\star = 0.59$. A family of limit cycles (Hopf bifurcations) appear around $E(0.59, 0.5)$. The variables v_1 and v_2 is about to produce periodic vibration around the numbers 0.59 and 0.5, respectively.

Figure 28 demonstrates the intercorrelations among the variables v_1, v_2 and the time t.

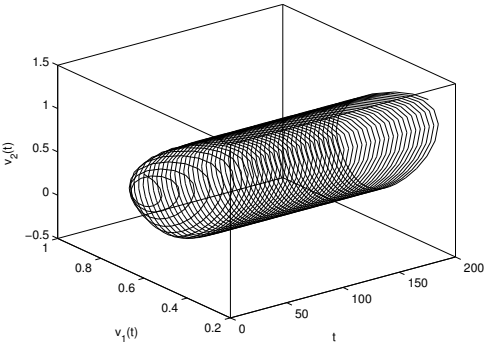

Figure 28. The three-dimensional space of model (99) concerning $\vartheta = 0.65 > \vartheta_\star = 0.59$. A family of limit cycles (Hopf bifurcations) appear around $E(0.59, 0.5)$. The variables v_1 and v_2 is about to produce periodic vibration around the numbers 0.59 and 0.5, respectively. It shows the intercorrelations among variables v_1, v_2 and the time t.

The bifurcation figures of model (99) are also presented in Figures 29-30.

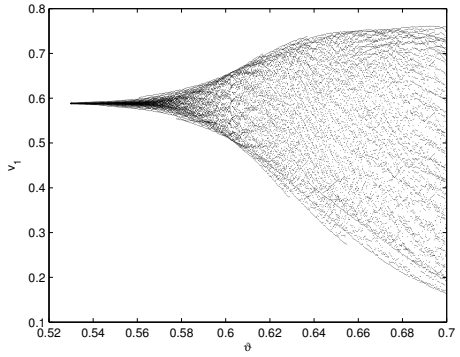

Figure 29. The bifurcation graph of model (99): ϑ versus v_1. It shows that the bifurcation value $\vartheta_\star \approx 0.59$.

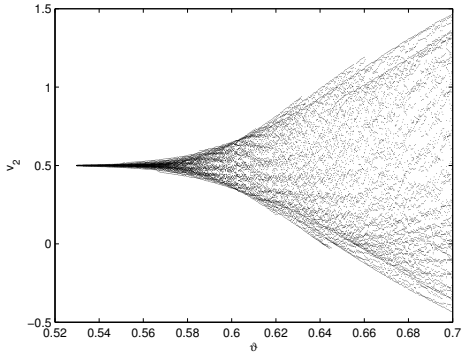

Figure 30. The bifurcation graph of model (99): ϑ versus v_2. It shows that the bifurcation value $\vartheta_\star \approx 0.59$.

8 Conclusions

How to build a proper dynamical model to depict the change rule of the concentrations of the various chemical substance has become an all-important subject in chemistry. Relying on the previous research, we set up a novel fractional-order delayed glycolytic oscillator model. The properties involving the existence and uniqueness, boundedness, non-negativeness of the solution to fractional-order delayed glycolytic oscillator model are

systematically analyzed. Making good use of Laplace transform, the stability theory and bifurcation knowledge of fractional differential system, a new delay-independent criterion on the stability and the appearance of bifurcation of the fractional-order delayed glycolytic oscillator model is presented. Designing skillfully proper delayed-feedback controller and PD^{α} controller, we are succeed in regulating the stability domain and the time of appearance of bifurcation for the fractional-order delayed glycolytic oscillator model. The gained results of this work own momentous theoretical guiding value in adjusting the concentration of fructose-6-phosphate and the concentration of adenosine diphosphate in chemistry. The study method is also exploited to seek bifurcation control aspect in plentiful delayed dynamical systems in various fields.

***Acknowledgment*:** The authors would like to thank the referees and the editor for helpful suggestions incorporated into this paper.

References

[1] A. Q. Khan, Neimark-Sacker bifurcation of a two-dimensional discrete-time chemical model, *Math. Prob. Eng.* **2020** #3936242.

[2] Z. U. A. Zafar, K. Rehan, M. Mushtaq, M. Rafiq, Numerical modeling for non-linear biochemical reaction networks, *Iran. J. Math. Chem.* **8** (2017) 413–423.

[3] Q. Din, K. Haider, Discretization, bifurcation analysis and chaos control for Schnakenberg model, *J. Math. Chem.* **58** (2020) 1615–1649.

[4] D. Kim, M. S. Lee, S. B. Yun, On the positivity of an auxiliary function of the BGK model for slow chemical reactions, *Appl. Math. Lett.* **113** (2021) #106841.

[5] J. J. Wang, Y. F. Jia, Analysis on bifurcation and stability of a generalized Gray-Scott chemical reaction model, *Phys. A* **528** (2019) #121394.

[6] L. Wang, D. Q. Jiang, G. S. K. Wolkowicz, Global asymptotic behavior of a multi-species stochastic chemostat model with discrete delays, *J. Dyn. Diff. Eq.* **32** (2020) 849–872.

[7] G. H. Guo, B. F. Li, X. L. Lin, Hopf bifurcation in spatially homogeneous and inhomogeneous autocatalysis models, *Comput. Math. Appl.* **67** (2014) 151–163.

[8] Y. F. Jia, Y. Li, J. H. Wu Qualitative analysis on positive steady-states for an autocatalytic reaction model in thermodynamics, *Discr. Contin. Dyn. Syst. Ser. A* **37** (2017) 4785–4813.

[9] C. J. Xu, C. Aouiti, Z. X. Liu, P. L. Li, L. Y. Yao, Bifurcation caused by delay in a fractional-order coupled Oregonator model in chemistry, *MATCH Commun. Math. Comput. Chem.* **88** (2022) 371–396.

[10] Q. Din, Dynamics and Hopf bifurcation of a chaotic chemical reaction model, *MATCH Commun. Math. Comput. Chem.* **88** (2022) 351–369.

[11] C. J. Xu, W. Zhang, C. Aouiti, Z. X. Liu, P. L. Li, Bifurcation dynamics in a fractional-order Oregonator model including time delay, *MATCH Commun. Math. Comput. Chem.* **87** (2022) 397–414.

[12] X. X. Qie, Q. B. Ji, Computational analysis and bifurcation of regular and chaotic Ca^{2+} oscillations, *Math.* **9** (2021) #3324.

[13] Q. Din, T. Donchev, D. Kolev, Stability, bifurcation analysis and chaos control in chlorine dioxide-iodine-malonic acid reaction, *MATCH Commun. Math. Comput. Chem.* **79** (2018) 577–606.

[14] R. H. Garrett, C. M. Grisham, *Biochemistry*, Saunder's College Pub., Philadelphia, 1999.

[15] J. M. Berg, J. L. Tymoczko, L. Stryer, *Biochemistry*, Macmillan, New York, 2002.

[16] T. Dandekar, S. Schuster, B. Snel, M. Huynen, P. Bork, Pathway alignment: application to the comparative analysis of glycolytic enzymes, *Biochem. J.* **343** (1999) 115–124.

[17] A. Boiteux and B. Hess, Design of glycolysis, *Phil. Trans. Royal Soc. London B* **293** (1981) 5–22.

[18] C. J. Xu, M. X. Liao, Bifurcation analysis of an autonomous epidemic predator- prey model with delay, *Ann. Mat. Pura Appl.* **193** (2014) 23–38.

[19] C. J. Xu, Q. M. Zhang, On the chaos control of the Qi system, *J. Eng. Math.* **90** (2015) 67–81.

[20] C. J. Xu, Y. S. Wu, Bifurcation and control of chaos in a chemical system, *Appl. Math. Model.* **39** (2015) 2295–2310.

[21] C. J. Xu, Z. X. Liu, L. Y. Yao, C. Aouiti, Further exploration on bifurcation of fractional-order six-neuron bi-directional associative memory neural networks with multi-delays, *Appl. Math. Comput.* **410** (2021) #126458.

[22] C. J. Xu, W. Zhang, Z. X. Liu, P. L. Li, L. Y. Yao, Bifurcation study for fractional-order three-layer neural networks involving four time delays, *Cogn. Comput.* **14** (2022) 714–732.

[23] C. J. Xu, D. Mu, Y. L. Pan, C. Aouiti, Y. C. Pang, L. Y. Yao, Probing into bifurcation for fractional-order BAM neural networks concerning multiple time delays, *J. Comput. Sci.* **62** (2022) #101701.

[24] C. J. Xu, Z. X. Liu, M. X. Liao, L. Y. Yao, Theoretical analysis and computer simulations of a fractional order bank data model incorporating two unequal time delays, *Expert Syst. Appl.* **199** (2022) #116859.

[25] X. J. Yang, C. D. Li, Q. K. Song, J. Y. Chen, J. J. Huang, Global Mittag-Leffler stability and synchronization analysis of fractional-order quaternion-valued neural networks with linear threshold neurons, *Neural Netw.* **105** (2018) 88–103.

[26] B. Ghanbari, S. Djilali, Mathematical analysis of a fractional-order predator-prey model with prey social behavior and infection developed in predator population, *Chaos Solitons Fract.* **138** (2020) #109960.

[27] C. J. Xu, Z. X. Liu, C. Aouiti, P. L. Li, L. Y. Yao, J. L. Yan, New exploration on bifurcation for fractional-order quaternion-valued neural networks involving leakage delays, *Cogn. Neurodyn.* **16** (2022) 1233–1248.

[28] C. J. Xu, W. Zhang, C. Aouiti, Z. X. Liu, L. Y. Yao, Further analysis on dynamical properties of fractional-order bi-directional associative memory neural networks involving double delays, *Math. Meth. Appl. Sci.* **45** (2022) 11736–11754.

[29] F. B. Yousef, A. Yousef, C. Maji, Effects of fear in a fractional-order predator-prey system with predator density-dependent prey mortality, *Chaos Solitons Fract.* **145** (2021) #110711.

[30] B. Ghanbari, S. Djilali, Mathematical analysis of a fractional-order predator-prey model with prey social behavior and infection developed in predator population, *Chaos Solitons Fract.* **138** (2020) #109960.

[31] M. Shafiya, G. Nagamani, New finite-time passivity criteria for delayed fractional-order neural networks based on Lyapunov function approach, *Chaos Solitons Fract.* **158** (2022) #112005.

[32] H. L. Tan, J. W. Wu, H. B. Bao, Event-triggered impulsive synchronization of fractional-order coupled neural networks, *Appl. Math. Comput.* **429** (2022) #127244.

[33] C. J. Xu, M. X. Liao, P. L. Li, Y. Guo, Z. X. Liu, Bifurcation properties for fractional order delayed BAM neural networks, *Cogn.Comput.* **13** (2021) 322–356.

[34] S. S. Xiao, Z. S. Wang, C. L. Wang, Passivity analysis of fractional-order neural networks with interval parameter uncertainties via an interval matrix polytope approach, *Neurocomputing* **477** (2022) 96–103.

[35] X. B. Nie, P. P. Liu, J. L. Liang, J. D. Cao, Exact coexistence and locally asymptotic stability of multiple equilibria for fractional-order delayed Hopfield neural networks with Gaussian activation function, *Neural Netw.* **142** (2021) 690–700.

[36] K. Udhayakumar, F. A. Rihan, R. Rakkiyappan, J. D. Cao, Fractional-order discontinuous systems with indefinite LKFs: An application to fractional-order neural networks with time delays, *Neural Netw.* **145** (2022) 319–330.

[37] F. H. Zhang, T. W. Huang, Q. J. Wu, Z. G. Zeng, Multistability of delayed fractional-order competitive neural networks, *Neural Netw.* **140** (2021) 325–335.

[38] N. Padmaja, P. Balasubramaniam, New delay and order-dependent passivity criteria for impulsive fractional-order neural networks with switching parameters and proportional delays, *Neurocomputing* **454** (2021) 113–123.

[39] C. J. Xu, M. X. Liao, P. L. Li, L. Y. Yao, Q. W. Qin, Y. L. Shang, Chaos control for a fractional-order Jerk system via time delay feedback controller and mixed controller, *Fract. Fractional* **5** (2021) #257.

[40] P. L. Li, J. L. Yan, C. J. Xu, Y. L. Shang, Dynamic analysis and bifurcation study on fractional-order tri-neuron neural networks incorporating delays, *Fract. Fractional***6** (2022) #161.

[41] C. J. Xu, D. Mu, C. Aouiti, Z. X. Liu, Q. W. Qin, L. Y. Yao, M. Hou, Bifurcation anti-control technique in a fractional-order stable

finance model, *Asian J. Control* (2022) **doi:** https://doi.org/10.1002/asjc.2865

[42] F. A. Rihan, C. Rajivganthi, Dynamics of fractional-order delay differential model of prey-predator system with Holling-type III and infection among predators, *Chaos Solitons Fract.* **141** (2020) #110365.

[43] C. D. Huang, J. D. Cao, M. Xiao, A. Alsaedi, T. Hayat, Bifurcations in a delayed fractional complex-valued neural network, *Appl. Math. Comput.* **292** (2017) 210–227.

[44] C. D. Huang, J. Wang, X. P. Chen, J. D. Cao, Bifurcations in a fractional-order BAM neural network with four different delays, *Neural Netw.* **141** (2021) 344–354.

[45] I. Podlubny, *Fractional Differential Equations*, Academic Press, New York, 1999.

[46] C. D. Huang, J. D. Cao, M. Xiao, A. Alsaedi, T. Hayat, Bifurcations in a delayed fractional complex-valued neural network, *Appl. Math. Comput.* **292** (2017) 210–227.

[47] Z. Odibat, N. Shawagfeh, Generalized Taylor's formula, *Appl. Math. Comput.* **186** (2007) 286–293.

[48] D. Matignon, Stability results for fractional differential equations with applications to control processing, *Comput. Engin. Sys. Appl.* **2** (1996) 963–968.

[49] W. H. Deng, C. P. Li, J. H. Lü, Stability analysis of linear fractional differential system with multiple time delays, *Nonlinear Dyn.* **48** (2007) 409–416.

[50] H. L. Li, L. Zhang, C. Hu, Y. L. Jiang, Z. D. Teng, Dynamical analysis of a fractional-order predator-prey model incorporating a prey refuge, *J. Appl. Math. Comput.* **54** (2017) 435–449.

[51] Q. S. Sun, M. Xiao, B. B. Tao, Local bifurcation analysis of a fractional-order dynamic model of genetic regulatory networks with delays, *Neural Proc. Lett.* **47** (2018) 1285–1296.